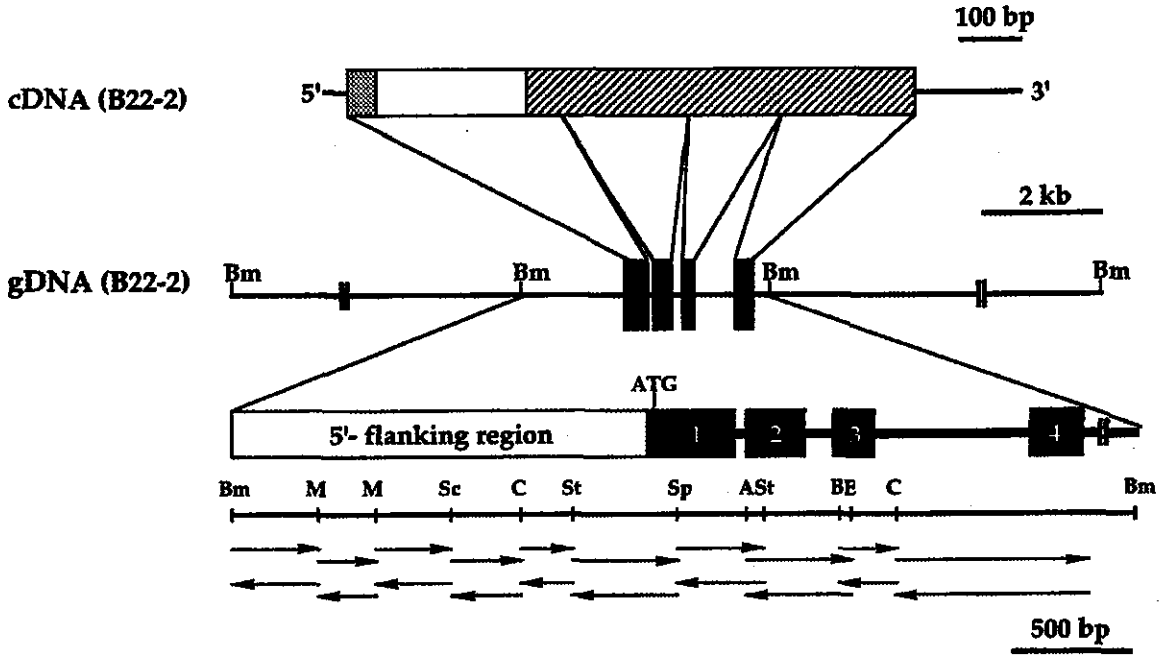

Fig. 1. Genomic organisation of *Fasciola gigantica* cathepsin L gene and sequencing strategy. In the cDNA, dotted, open and striped boxes indicate regions encoding the signal sequence, pro-peptide and mature enzyme domains, respectively. In the genomic clone, closed boxes indicate exons and solid bars denote introns. Bm, *Bam*HI; M, *Mva*I; C, *Cla*I; St, *Sty*I; Sp, *Ssp*I; A, *Age*I; E, *Eco*O109I; B, *Bsm*I. Arrows indicate the direction of sequencing.

2.7. Expression and refolding of the recombinant procathepsin L and pro-peptide deleted cathepsin L

Two cDNAs encoding *F. gigantica* procathepsin L and pro-peptide deleted cathepsin L (B22-2) were amplified by PCR using cDNA as described above. Primer sets used were pro 5′-primer/3′-primer, and mCL 5′-primer/3′-primer based on the nucleotide sequence of *Fg CATL* (B22-2, AB010923). PCR was performed using AmpliTaq DNA polymerase (Perkin Elmer) as follows: 95 °C, 1 min; 55 °C, 1 min; 72 °C, 2 min; 35 cycles. The PCR product was subcloned into pT7Blue T-vector (Novagene, USA) and sequenced. cDNA corresponding to B22-2 clone was inserted into the pGEX-4T-1 expression vector (Pharmacia Amersham Biotech), and designated pGEX/*proCATL* for procathepsin L or pGEX/*mCATL* for pro-peptide deleted cathepsin L. Each construct was then introduced into BL21 *Escherichia coli* strain (Novagene). The expression of glutathione *S*-transferase (GST) fused with either procathepsin L or pro-peptide deleted cathepsin L was induced by adding a final concentration of 1 mM isopropyl-β-D(−)thiogalactopyranoside (IPTG) for 2–3 h at 37 °C.

Cells from 1 l culture were harvested, and the cell pellet was resuspended in chilled PBS containing 0.1% Triton X-100 and 1% sarcosine, and then sonicated using a sonifier (Branson). The resulting suspensions were centrifuged at 15,000 rpm for 10 min, and the pellets were rinsed in several times in PBS and resuspended in 20 ml of 50 mM Tris–HCl, pH 8.0, containing 50 mM NaCl, 5 mM EDTA and 10 mM dithiothreitol (DTT). Urea was added to a final concentration of 8 M to solubilise the suspension completely. Refolding was performed according to a previously described procedure (Smith and Gottesman, 1989). Briefly, the urea-solubilised GST-fusion proteins were slowly added dropwise (2 ml/h) into 400 volumes of 50 mM potassium phosphate buffer, pH 10.7, containing 5 mM EDTA, 0.1 mM oxidised glutathione and 1 mM reduced glutathione to a final protein concentration of approximately 10 μg/ml, and stirred at 4 °C overnight. The solutions of solubilised proteins were then adjusted to pH 8.0 and concentrated to 1/300 of the original volume using an Amicon cell ultrafiltration unit. After concentration, the solutions were centrifuged briefly for further experiments.

2.8. Purification of recombinant and native cathepsins L

The refolded GST-fusion proteins were cleaved with thrombin to remove GST according to the manufacturer's manual and the recombinant procathepsin L was dialysed against 10 mM Na_2HPO_4/1.8 mM KH_2PO_4, pH 8.0, containing 140 mM NaCl, 2.7 mM KCl and 4 M urea, and the resulting solution were applied to a Sephacryl S-200 HR gel chromatography column (1.5 × 120 cm) equilibrated with same buffer. The eluates were analysed by SDS–PAGE (Laemmli, 1970). In order to compare the activities of recombinant and native cathepsin L, native cathepsin L was partially purified from *F. gigantica* adult worms. Briefly, 1.5 g of lyophilised parasites were homogenised

in 40 mM sodium acetate buffer, pH 3.9, containing 150 mM NaCl, 1 mM EDTA, and 1 mM DTT. The resulting supernatant was dialysed against the same buffer and applied to TSK-Gel 3000SW column (21.5 × 600 mm) in a high-performance liquid chromatograph (Shimadzu, Model LC-6A). Fractions showing activities toward carbobenzoxyl-L-phenylalanyl-L-arginine 4-methyl-coumaryl amide (Z-Phe-Arg-MCA, Peptide Institute) were pooled for further experiments.

2.9. Enzyme assay

Cathepsin L activity was assayed according to the method of Barrett and Kirschke, (1981). Briefly, 10 μl of recombinant or native cathepsin L in 80 μl of 80 mM sodium acetate buffer, pH 5.5, containing 8 mM L-cysteine and 4 mM EDTA were preincubated at 37 °C for 5 min, and the enzyme reaction was initiated by adding 10 μl of 1 mM Z-Phe-Arg-MCA at 37 °C for 10 min, and terminated by adding 100 μl of 5% SDS. The 7-amino-4-methyl-coumarin released was measured using a fluorescence spectrophotometry (Hitachi, Model 850) at an excitation wavelength of 370 nm and emission wavelength of 460 nm.

2.10. NH_2-terminal sequencing of recombinant procathepsin L, pro-peptide deleted- and processed cathepsins L

Both GST-fused procathepsin L and cathepsin L were cleaved with thrombin, electrophoresed, and then were blotted onto a PVDF membrane for NH_2-terminal sequencing according to the method of Matsudaira (1987). The NH_2-terminal amino acid sequence of recombinant cathepsin L processed in vitro was also electrophoresed. The target bands were cut and then applied to a Protein Sequencer (Applied Biosystems, Model 477A).

2.11. Protein assay

The protein content was determined by the Bradford method using a protein assay kit (BioRad).

3. Results

3.1. Structure of the F. gigantica cathepsin L gene

Recombinant clones (6×10^4) were screened with a digoxigenin-labelled *Fasciola* cathepsin L cDNA probe (Yamasaki and Aoki, 1993), and a positive clone (B22-2) with a 16 kb DNA fragment was isolated. The DNA fragment was digested with *Bam*HI, a 4.3 kb fragment hybridised with the probe was obtained, and 3,766 bp including a 5′-flanking region of the fragment were determined. Fig. 1 illustrates the schematic structure of the *F. gigantica* cathepsin L gene (*Fg-CATL*) and sequence strategy. The nucleotide and deduced amino acid sequences of the *Fg-CATL* (B22-2, AB010923) are shown in Fig. 2. The gene consists of four exons and three introns spanning approximately 2.0 kb in the genome. The length of each exon varies from 378, 222, 158, and 217 bp in exons 1, 2, 3 and 4, respectively. Exon 1 encodes 15 amino acid residues of the signal sequence, 90 amino acid residues of the pro-region, and the first 21 residues of the mature enzyme. The remainder of the mature enzyme is encoded by exons 2–4. Cys^{27}, His^{164} and Asn^{184}, which form the catalytic triad in the active sites, are encoded in exons 2 and 4, respectively. The intron breakpoints are not found at the junction of the pre-, propeptide and mature enzyme domains, indicating that the gene structure does not correspond to the functional units of the protease as well other cathepsin L (Ishidoh et al., 1989). The length of each intron varies from 53, 163 and 694 bp in introns 1, 2 and 3, respectively. Furthermore, introns 1 and 2 interrupt the open reading frame between two codons (type 0), whereas intron 3 interrupts the coding sequence after the second nucleotide of a codon (type 2) (Patthy, 1987). The exon–intron boundary sites, determined by comparison with the cDNA sequence, are all consistent with the GT-AG rule (Breathnach and Chambon, 1981). In the 5′-flanking region of *Fg-CATL*, two putative TATA boxes were found 58 and 68 nucleotides upstream of a transcription initiation site (Fig. 2), one of which might be involved in the transcription activity of the gene. However, no CCAAT (CAT box) that enhances the transcription activity was found in this region, as in the case of *Spirometra erinacei* cathepsin L gene (Liu et al., 1996).

Southern blot analysis of *F. gigantica* genomic DNA revealed two or three signals in each of the enzymes used (Fig. 3). Apart from the genomic clone (B22-2), another1.8-kb *Fg-CATL* was co-amplified (data not shown) when *Fg-CATL* (B22-2) was amplified by PCR using genomic DNA for probe preparation. Sequence analysis revealed the gene, termed *Fg-CATL* (B7-3, accession number AB010924), is distinct from *Fg-CATL* (B22-2) at the nucleotide and amino acid levels. The remarked difference was observed in length and sequence in the third intron, the sizes of 582 and 694 bp were in the B22-2 and B7-3 *Fg-CATLs*, respectively. In Northern blot analysis, an approximately 1.0 kb transcript was detected when a B22-2 cathepsin L cDNA was used as a probe (Fig. 4). Sequence analysis of the 5′-untranslated region of the *Fg-CATL* mRNAs revealed a predicted transcription initiation site at an adenine 14 nucleotides upstream of the translation initiation site.

3.2. Amino acid sequence characterisation of F. gigantica cathepsin L and homology with other known cathepsin L

Fig. 5 shows the aligned sequences and intron insertion positions of cathepsins L from *F. gigantica*, *S. erinacei* plerocercoid (Liu et al., 1996), shrimp (Boulay et al., 1998) and rat (Ishidoh et al., 1989). The amino acid sequences of *F. gigantica* cathepsins L (Fg CATL B22-2 and B7-3) are homologous to those of cathepsins L from other eukaryotes. The regions containing the Cys^{27}, His^{164}

and Asn[184] residues at the active sites are highly conserved. Since it is confirmed that a cathepsin L (B22-2) is expressed in the *F. gigantica* adult worms, the cathepsin L described here is Fg CATL (B22-2). The ERFNIN motif (Karrer et al., 1993) was found, but the first amino acid of the motif, Glu, was replaced by Val (grey box in Fig. 2 and overlined a in Fig. 5). Most recently, an evolutionarily conserved tripartite tryptophan motif has been identified in cathepsin L-like

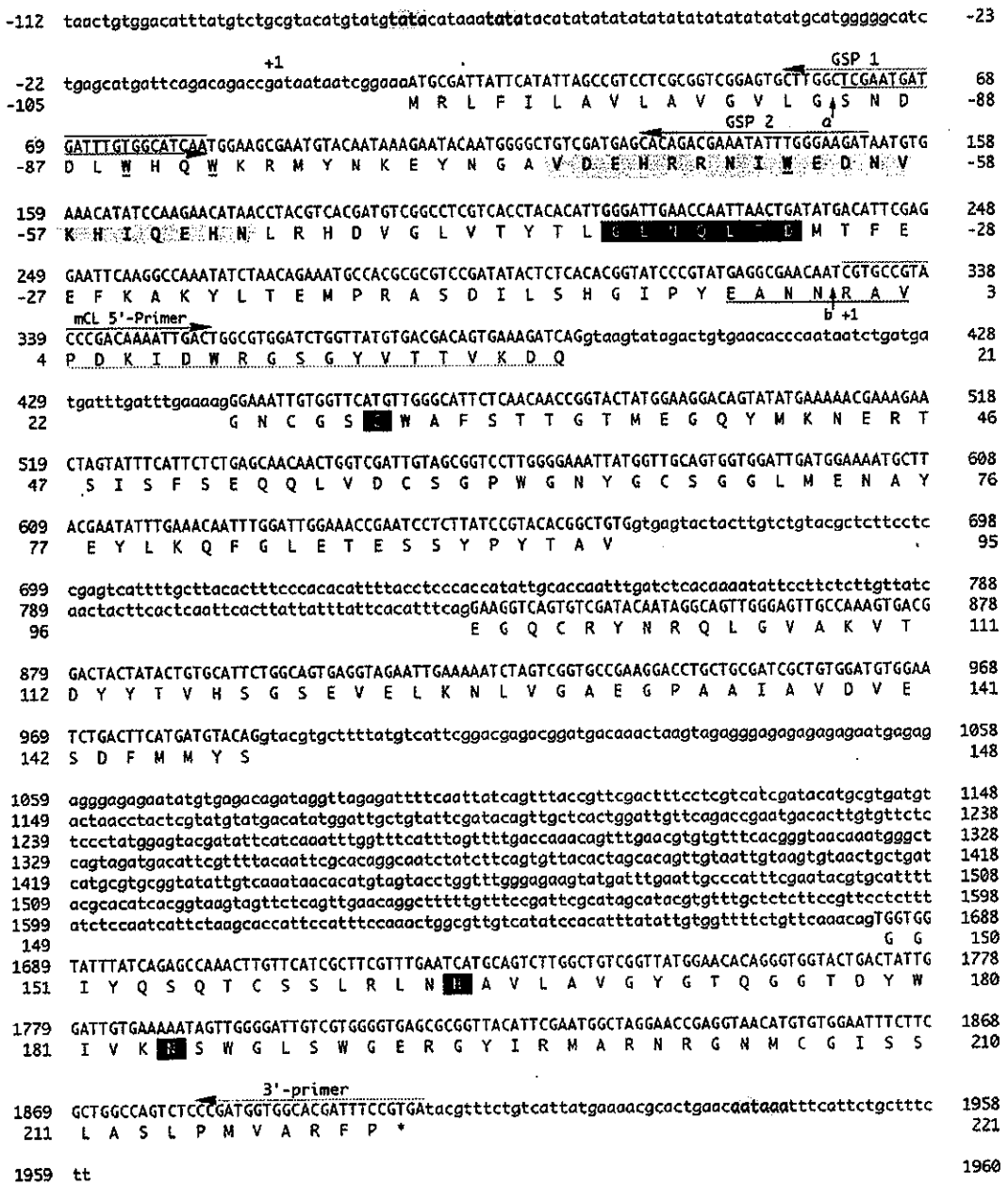

Fig. 2. Nucleotide and deduced amino acid sequences of *Fasciola gigantica* cathepsin L (B22-2). Nucleotides are numbered from the transcription initiation site (+1). The amino acid sequence deduced from the nucleotide sequence is shown below the nucleotide sequences and is numbered from the first amino acid (Arg^{+1}) of the mature enzyme. Intron sequences are shown in lowercase letters. Putative TATA boxes and a polyadenylation addition signal are in grey boxes. The asterisk indicates a translation termination codon. Arrows a and b indicate putative cleavage sites for signal sequence and the pro-peptide. Active site residues (Cys^{27}, His^{164} and Asn^{184}) are in black boxes. The ERFNIN motif (Val^{-70} to Asn^{-51}) and the putative intramolecular processing motif (Gly^{-38} to Asp^{-32}) are in grey and black boxes, respectively. The three aromatic residues (Trp^{-85}, Trp^{-82} and Trp^{-62}) in a tripartite tryptophan motif are underlined. The NH_2-terminal sequence of the recombinant cathepsin L processed in vitro is underlined (Glu^{-4} to Gln^{21}). GSP 1 and 2 primers were used for 5′-rapid amplification of cDNA ends. The underlined region (nucleotides 60–83), mCL 5′- and 3′-primers were used to amplify the procathepsin L and the pro-peptide deleted cathepsin L cDNAs, respectively.

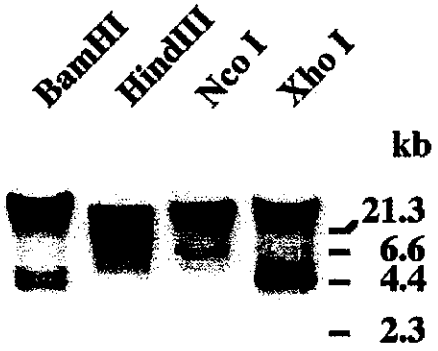

Fig. 3. Southern blot analysis of *Fasciola gigantica* cathepsin L gene. *Fasciola gigantica* genomic DNA (1.2 μg) was digested completely with either *Bam*HI, *Hin*dIII, *Nco*I or *Xho*I, electrophoresed, transferred, and then hybridised with a digoxigenin-labelled *Fasciola* preprocathepsin L genomic clone as a probe. Digoxigenin-labelled DNA size markers are indicated on the right.

cysteine proteases (Kreusch et al., 2000). In *F. gigantica* cathepsin L, this motif is completely conserved (double-underlined in Fig. 2 and closed triangles in Fig.5). Another sequence motif, GNFD, which may be involved in intramolecular processing in propapain (Vernet et al., 1995), is also highly conserved although Phe^{-38} is replaced by Leu^{-34} in *F. gigantica* cathepsin L (black box in Fig.2 and overline b in Fig. 5). As shown in Fig.2, *Fg-CATL* has three introns, two of which is located in the same position as in rat, and one of which is same as in rat and shrimp cathepsins L (Fig. 5). Interestingly, there is no common intron insertion position between *Fg-CATL* and *S. erinacei* plerocercoid cathepsin L gene though these parasites belong to taxonomically the phylum platyhelminths. The region around the catalytic site Cys^{27} is generally split by an intron. In *F. gigantica* cathepsin L, the junction is located close to the Cys^{27} residue, as in rat cathepsin L, whereas the sites in *S. erinacei* and shrimp cathepsins L are located before and after the Cys^{27} residue, respectively.

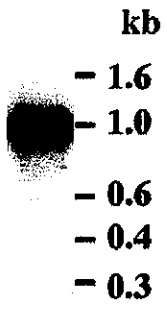

Fig. 4. Northern blot analysis of a *Fasciola gigantica* cathepsin L transcript. mRNA (0.6 μg) was electrophoresed in a 1% agarose gel containing 50% formamide, transferred to a nylon membrane, hybridised with a digoxigenin-labelled *Fasciola* cathepsin L cDNA (B22-2) as a probe, and exposed to X-ray film for 5 min. Digoxigenin-labelled RNA size markers are indicated on the right.

Table 1 shows the amino acid homologies of Fg CATL (B22-2) with cathepsins L from parasitic platyhelminths, a shrimp and a mammal. Fg CATL (B22-2) is highly homologous with *F. gigantica* cathepsin L (Fg CATL-A, Grams et al., 2001) and *F. hepatica* cathepsin L1 (Fh CATL-1, Roche et al., 1997) with homologies of 94.8 and 91.1%, respectively, not but with *F. gigantica* cathepsin L (Fg CATL-D, Grams et al., 2001) and *F. hepatica* cathepsin L2 (Fh CATL-2, Dowd et al., 1997). Fg CATL (B22-2) shows lower homologies (42.1–44.8%) with those of a larval cestode, schistosomes, shrimp and rat.

3.3. Phylogenetic analysis of cathepsin L from F. gigantica

A phylogenetic analysis of 25 members of the papain superfamily revealed that the cathepsins L from *F. gigantica* form a monophyletic cluster with those of *F. hepatica* (Fig. 6). The two subgroups, representing by Fg CATL-D and Fh CATL-2, and by Fg CATL (B22-2) and Fh CATL-1, are seemed to be similar divergence between each other that do the cathepsins L of schistosomes and *F. hepatica*. Interestingly, cathepsins L from the liver flukes form a separate clade that contains the cathepsins L from *Schistosoma japonicum* (Sj CATL-2, Day et al., 1995), *Schistosoma mansoni* (Sm CATL-2, Dalton et al., 1996a) and *S. erinacei* that belong to the same phylum as well as the liver flukes.

3.4. Expression and in vitro processing of the recombinant procathepsin L

Fig. 7 shows SDS–PAGE analysis of proteins produced in non-induced and induced cells carrying either pGEX/*proCATL* or pGEX/*mCATL*. GST-procathepsin L and GST-cathepsin L were expressed as insoluble proteins with molecular masses of 64 and 52 kDa, respectively. The fusion proteins were solubilised in 8 M urea and renatured by the procedure described in Section 2. The refolded GST-fusion proteins were then treated with thrombin to separate target proteins from GST. Finally, 38 and 26 kDa proteins were separated on SDS–PAGE, and the sequences of the NH_2-terminal first 10 amino acids of each protein coincided completely with those deduced from the procathepsin L and mature form cathepsin L cDNAs.

Once *F. gigantica* procathepsin L was refolded, it showed increasing enzyme activities against a fluorogenic substrate, Z-Phe-Arg-MCA, over time. As shown in Fig. 8, the hydrolysing activities increased remarkably at pH 4.5–5.5. However, the enzyme activities were lower at other pH and no activity was detected at pH 8.0. The processing occurs by a

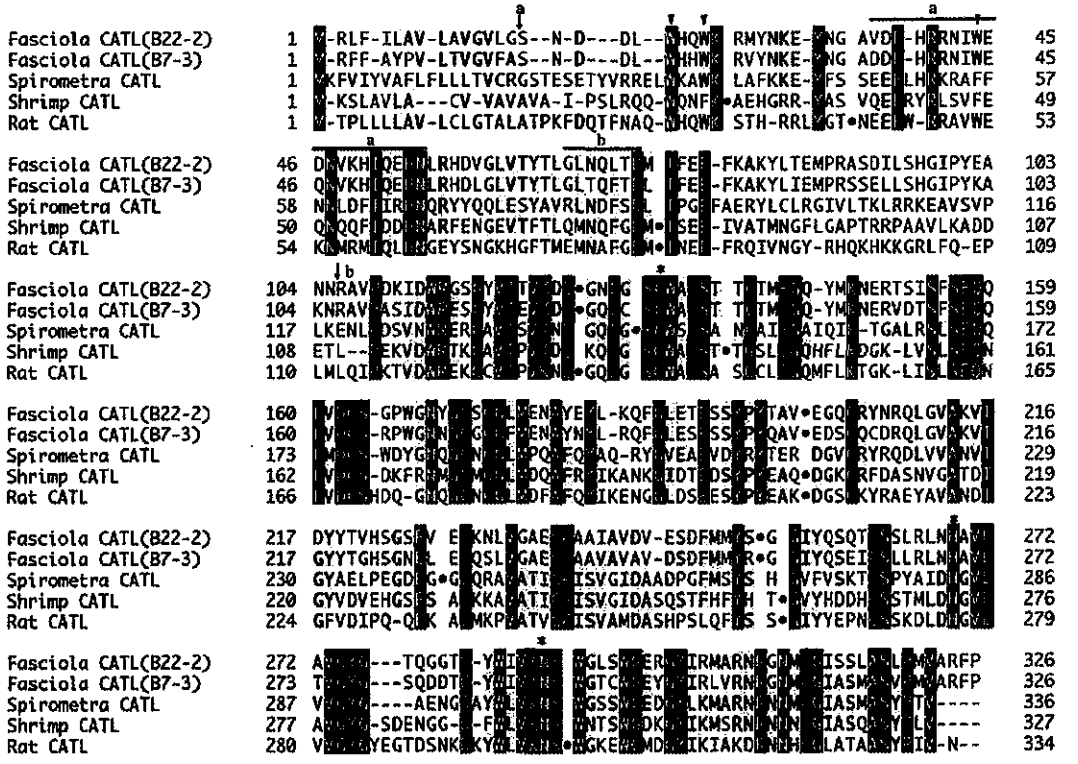

Fig. 5. Alignment of the predicted amino acid sequences and intron insertion positions of cathepsins L from *Fasciola gigantica*, *Spirometra erinacei*, shrimp and rat. Cathepsin L genes whose intron insertion positions are determined are selected. The catalytic triad residues are marked with asterisks, and gaps (-) are introduced to maximise alignment. Arrows a and b indicate the putative cleavage sites of the signal sequence and pro-peptide of *F. gigantica* cathepsin L, respectively. Intron insertion positions are indicated by closed circles. The ERFNIN and the intramolecular processing motifs are shown by overlines a and b, respectively. The tripartite tryptophan residues are denoted by closed triangles. Identical amino acid residues are shown in black boxes.

pH-dependent autocatalytic mechanism in vitro and it seems to occur in multiple steps based on the results by Western blotting (data not shown). Interestingly, the processed active cathepsin L degraded GST in the reaction mixture after overnight incubation at pH 5.5. In addition, the processing reaction was completely inhibited in the presence of an irreversible inhibitor, E-64 (Fig. 8), indicating that the interaction with the prodomain of procathepsin L with the inhibitor results in the inhibition of autocatalysis of the enzyme.

The specific activity of the processed cathepsin L was 4,282 nmol/mg protein per minute, corresponding to 80% of that of native cathepsin L (5,308 nmol/mg protein per minute). K_m values for recombinant and native cathepsin L toward Z-Phe-Arg-MCA were 83.3 and 23.3 μM, respectively. The processed cathepsin L did not show any activities against Z-Arg-Arg-MCA, a substrate for cathepsin B, and Arg-MCA for cathepsin H as well as native *F. gigantica* cathepsin L (data not shown). Furthermore, the sequencing of the 26 kDa-processed cathepsin L revealed the NH_2-terminal to be Glu^{-4}-Ala^{-3}-Asn^{-2}-Asn^{-1}-Arg^{+1}-Val^{+2}-Pro^{+3}-Asp^{+4} (underlined in Fig. 2), corresponding to a four-amino-acid extension at the NH_2-terminal of native *F. gigantica* cathepsin L.

4. Discussion

We describe here the genomic structure and sequence analysis of *F. gigantica* cathepsin L and the in vitro processing of the recombinant *F. gigantica* procathepsin L. Sequence analysis revealed that *Fg-CATL* is as a basically similar structure to the other cathepsin L genes. However, *Fg-CATL* contains fewer introns compared with those of its mammalian counterparts and is a compact gene as in the case of cathepsin L from a platyhelminth *S. erinacei* (Liu et al., 1996). Previously sequenced cathepsin L genes from protozoan parasites are entirely devoid of any introns (Rosenthal and Nelson, 1992; Eakin et al., 1992). Regarding intron insertion positions, a junction close to the catalytic residue (Asn^{185}) found in rat cathepsin L is absent in *F. gigantica* cathepsin L. The junction between Val^{200} and Glu^{201} is conserved in shrimp and rat cathepsins L and in rat cathepsin H. It is interesting to note that the intron insertion positions are similar to those in mammalian and crustaceous cathepsins L rather than to those in the taxonomically closely related *S. erinacei*.

Southern blot analysis revealed that the *Fg-CATL* gene family comprises only a few copies. It was difficult to esti-

Table 1
Amino acid homologies among selected cathepsins L

	Fg CATL (B22-2)	Fg CATL (B7-3)	Fg CATL-A	Fg CATL-D	Fh CATL-1	Fh CATL-2	Se CATL	Sj CATL-2	Sm CATL-2	Shrimp CATL
Fg CATL (B22-2)[a]	100.0									
Fg CATL (B7-3)[a]	78.8	100.0								
Fg CATL-A[b]	94.8	81.3	100.0							
Fg CATL-D[b]	77.3	77.9	78.5	100.0						
Fh CATL-1[c]	91.1	80.1	93.6	77.3	100.0					
Fh CATL-2[d]	77.0	77.9	77.3	92.3	77.3	100.0				
Se CATL[e]	43.6	43.0	45.0	45.3	45.0	46.6	100.0			
Sj CATL-2[f]	43.9	43.6	44.6	44.6	44.9	43.4	43.6	100.0		
Sm CATL-2[g]	44.8	45.4	46.1	44.1	46.7	45.4	46.1	75.7	100.0	
Shrimp CATL[h]	44.5	41.3	45.4	43.6	45.1	43.9	46.2	40.4	44.6	100.0
Rat CATL[i]	42.1	40.5	43.0	39.4	43.4	41.9	46.0	40.1	44.7	51.5

[a] *Fasciola gigantica* cathepsin L descibed in the present study.
[b] *Fasciola gigantica* cathepsin L (Grams et al., 2001).
[c] *Fasciola hepatica* cathepsin L (Roche et al., 1997).
[d] *Fasciola hepatica* cathepsin L (Dowd et al., 1997).
[e] *Spirometra erinacei* cathepsin L (Liu et al., 1996).
[f] *Schistosoma japonicum* cathepsin L (Day et al., 1995).
[g] *Schistosoma mansoni* cathepsin L (Dalton et al., 1996a).
[h] *Penaeus vannamei* cathepsin L (Boulay et al., 1998).
[i] *Rattus norvegicus* cathepsin L (Ishidoh et al., 1989).

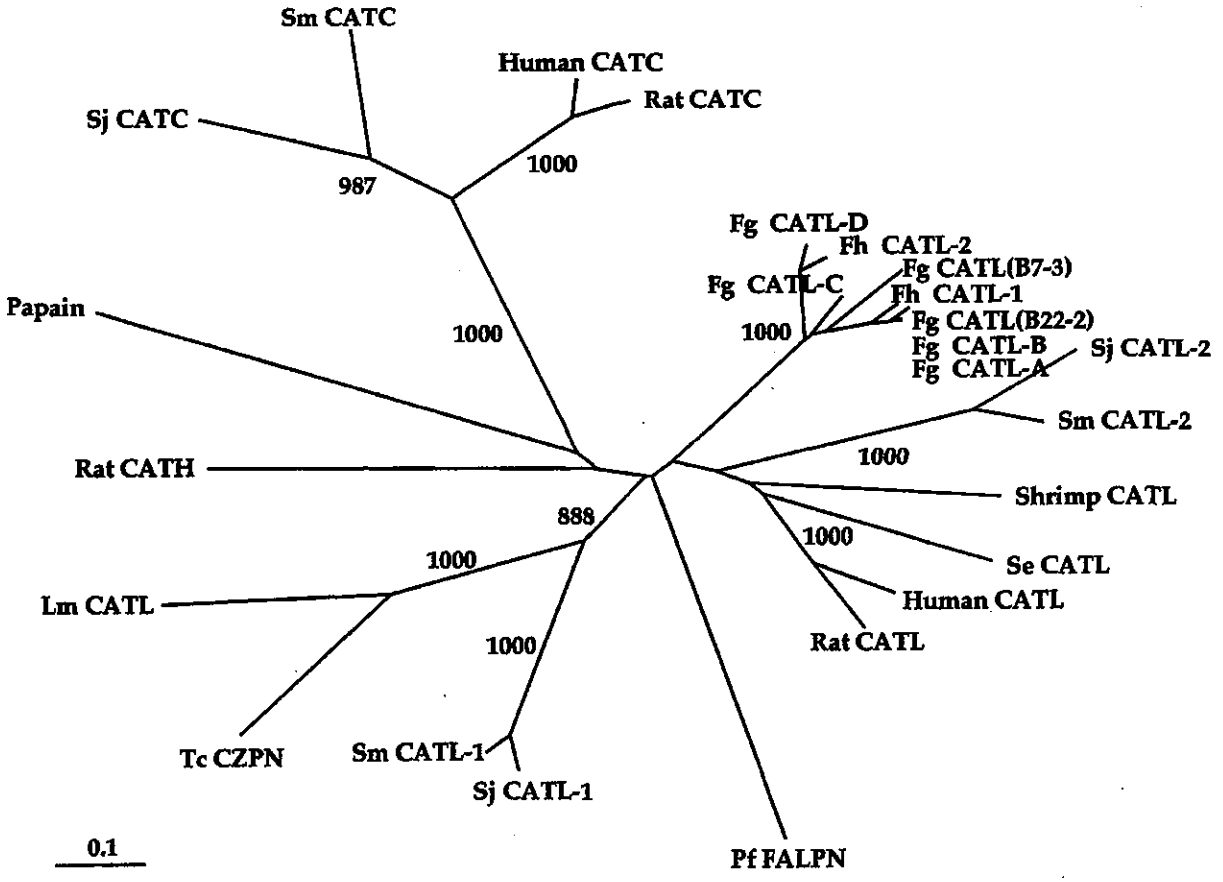

Fig. 6. Phylogenetic tree of cathepsins L from *Fasciola gigantica*, *Fasciola hepatica* and other organisms. Unrooted neighbour-joining tree was prepared using the amino acid sequences of representative members of the papain superfamily. Numbers adjacent to branches represent bootstrap values. The bar indicates the numbers of substitutions per site. The cathepsins L used were from *F. gigantica* (Fg CATL-A, AF112566, Fg CATL B-D, AF239264-6), *F. hepatica* (Fh CATL-1, U62288; Fh CATL-2, U62289), *Penaeus vannamei* (Shrimp CATL, Y14965), Rat (Rat CATL, Y00697), human (Human CATL, X12451), *Spirometra erinacei* (Se CATL, D63670), *Schistosoma mansoni* (Sm CATL-1, U07345; Sm CATL-2, Z32529), *Schistosoma japonicum* (Sj CATL-1, U38475; Sj CATL-2, U38476), *Plasmodium falciparum* (Pf FALPN, M81341), *Leishmania mexicana* (Lm CATL, Z14061), *Trypanosoma cruzi* (Tc CZPN, X54414) and papain (M15203).

mate exact copy numbers, but at least three copies exist. Grams et al. (2001) reported that a cathepsin L gene family comprising an estimated 10 related cathepsin L genes exists in *F. gigantica*. From these observations, it is obvious that cathepsin L genes form a gene family in the *F. gigantica* as in the cases of *F. hepatica* (Dowd et al., 1994; Heussler and Dobbelaere, 1994). This is similar to the degree of diversity reported for cathepsin L genes in *S. mansoni* (Dalton et al., 1996a) and a coleopteran insect, *Sitophilus zeamais* (Matsumoto et al., 1997). However, it is not clear why the closely related cathepsin L genes have been evolved in these liver flukes. Possibly, gene duplication of cathepsin L gene occurred in the common ancestry for both *F. gigantica* and *F. hepatica*. After species differentiation, cathepsin L genes might have been diversified by gene conversion in each *Fasciola* species. The existence of multiple cathepsin L genes may suggest that the cathepsin L family has diverse biological functions at different developmental stages or tissues although it is unclear whether multiple transcripts are translated into different cathepsins L. A cathepsin L derived from the B22-2 clone is expressed as a predominant enzyme in *F. gigantica* adult worms (data not shown) and can degrade host haemoglobin as a physiological substrate as in the case of *Fasciola* sp. (Yamasaki et al., 1989, 1992). However, the enzyme cannot be cleaved intact host erythrocyte membrane (unpublished data). As far as we examined, there is no direct evidence that another cathepsin L (B7-3) is expressed in the *F. gigantica* adult worms.

It is also known that a 37-nucleotide spliced leader sequence is added at the 5′-ends of *F. hepatica* mRNAs, indicating that *trans*-splicing is likely to be a common feature in trematodes and perhaps other flatworms (Davis et al., 1994). However, 5′-RACE or PCR results using a *F. hepatica* spliced leader primer did not support the feature mentioned above, indicating that *Fg-CATL* is transcribed by a *cis*-splicing mechanism. In the platyhelminth, it is interesting whether cysteine protease genes including cathepsin L are transcribed by *cis*-splicing fashion or not.

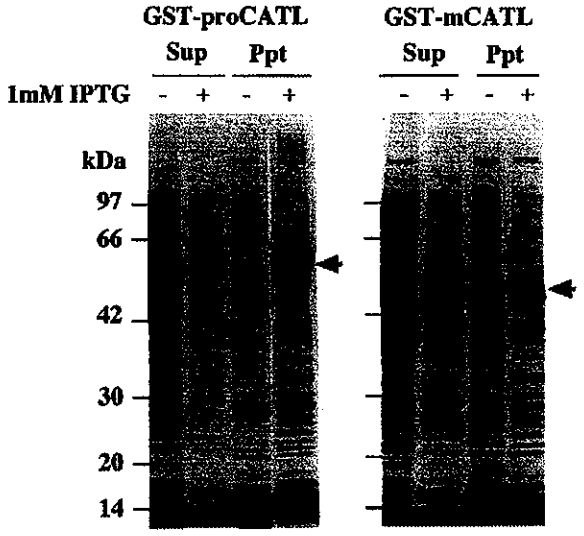

Fig. 7. SDS–PAGE analysis of recombinant procathepsin L and cathepsin L fused with glutathione *S*-transferase (GST) expressed in *Escherichia coli*. Proteins from non-induced and induced cells were subjected to SDS–PAGE (10–20% gradient gel) to monitor the expression of GST-fusion proteins. Arrows indicate GST fused with procathepsin L (64 kDa) and cathepsin L (52 kDa), respectively. Sup and Ppt are soluble and insoluble fractions, respectively. Size markers are indicated on the left.

In the pro-peptide regions of cysteine proteases belonging to a cathepsin L subfamily, a consensus sequence exists comprising conserved amino acids interspersed with variable ones, $EX_3RX_2(V/I)FX_2NX_3IX_3N$ (Karrer et al., 1993). The ERFNIN motif, which is considered to be a functional unit involved in the inhibition of enzyme activity, was found in *F. gigantica* cathepsin L, although the first amino acid of the motif, Glu, is replaced by Val. An evolutionarily conserved tripartite tryptophan motif has been identified in cathepsin L-like cysteine proteases (Kreusch et al., 2000). The motif was shown to be of importance for the maintenance of the prodomain structure of procathepsin S. X-ray crystallographic studies of human procathepsin L showed that cathepsin L-like cysteine proteases contain two α helices crossing each other and the three aromatic residues contribute to a small core surrounded by hydrophobic residues at the point of intersection (Coulombe et al., 1996). The tripartite tryptophan motif, Trp^{-85}, Trp^{-82} and Trp^{-62}, is completely conserved in *F. gigantica* cathepsin L, suggesting that the motif may play important roles in the maintenance of the prodomain structure.

The experiments using a recombinant procathepsin L revealed that the in vitro activation of procathepsin L occurs by pH-dependent autocatalysis. Furthermore, the NH_2-terminal sequencing revealed that the 26 kDa-processed cathepsin L has Glu^{-4}-Ala^{-3}-Asn^{-2}-Asn^{-1}-Arg^{+1}-Val^{+2}-Pro^{+3}-Asp^{+4}, corresponding to a four amino acid extension at the NH_2-terminal of native *F. gigantica* cathepsin L. The difference could be due to differences in the pH-dependent autocatalytic processing in vitro and the cleavage site specificity of the enzyme(s) involved in intracellular processing in vivo. In contrast to procathepsin L, the pro-peptide deleted recombinant cathepsin L showed no enzyme activity against any fluorogenic substrates. The GNFD motif in the prodomain of the propapain could participate in pH-dependent intramolecular processing (Vernet et al., 1995). A similar motif is found in *F. gigantica* procathepsin L, although Phe^{-38} in propapain is replaced by Leu^{-34} in *F. gigantica* cathepsin L. Considering the existence of a potential intramolecular processing motif in the pro-peptide region, it may be reasonable that pro-peptide deleted cathepsin L did not show any enzyme activity. A part of the pro-peptide is also essential for the proper folding of functional cathepsin L in *F. gigantica*. The pro-peptide also plays essential roles for protein folding, endoplasmic reticulum exit, stability, and mannose phosphorylation in mouse procathepsin L (Tao et al., 1994). As the function of the pro-peptide, Roche et al. (1999) reported that the pro-peptide of the *F. hepatica* cathepsin L (Fh CATL-1) showed a very potent and specific inhibition against the Fh CATL-1. This is considered that a part of the pro-peptide enters the substrate binding cleft in a reverse orientation to natural substrate and blocks access to the active site (Coulombe et al., 1996).

In contrast to mammalian cathepsin L, it is very interesting that *F. gigantica* cathepsin L lacks *N*-linked sugar moiety. It has been reported that a cathepsin L from Japa-

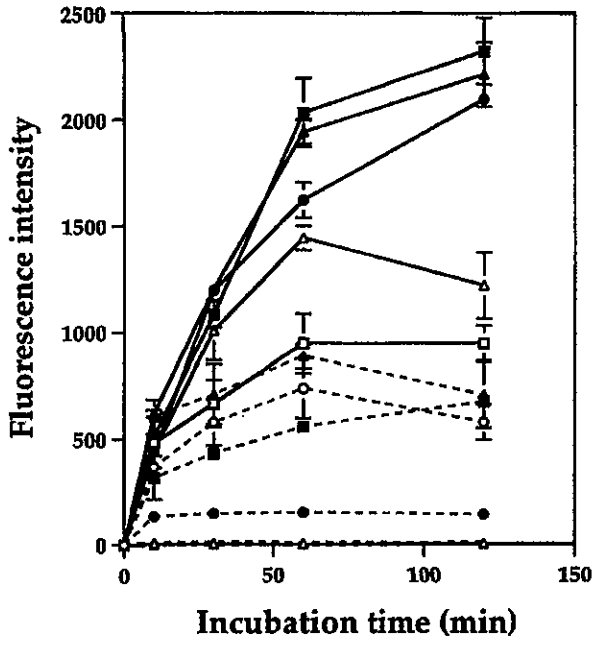

Fig. 8. In vitro processing of procathepsin L. The purified recombinant procathepsin L was preincubated at 37 °C in buffers of varying pH for the times indicated, and the hydrolysing activities against Z-Phe-Arg-MCA were assayed and plotted versus the corresponding preincubation time. pH 3.0 (- -○- -), pH 3.5 (- -▲- -), pH 4.0 (—□—), pH 4.5 (—▲—), pH 5.0 (—■—), pH 5.5 (—●—), pH 6.0 (—△—), pH 6.5 (- -■- -), pH 8.0 (- -●- -), pH 5.0 in the presence of E-64 (- -△- -). Each bar represents the average ± SD for two independent experiments.

nese *Fasciola* sp. localises in the secretory granules in intestinal epithelial cells of the worms (Yamasaki et al., 1992; Yamasaki and Aoki, 1993). This suggests that the intracellular transport mechanism of *F. gigantica* cathepsin L is different from those of mammalian cathepsins L. In order to clarify the function of the pro-peptide in the intracellular transport mechanism of *F. gigantica* cathepsin L, experiments using deletion mutants of *F. gigantica* procathepsin L fused with a green fluorescent protein are currently in progress.

Acknowledgements

We thank Professor Dr Takeshi Agatsuma for the molecular identification of the *Fasciola* parasite, and Naomi Mori, Koichi Kawakami and Mami Kaneko for technical assistance. This work was supported in part by grants-in-aid for Scientific Research from the Ministry of Education, Science, Culture and Sports, Japan (Nos. 05670241,07670291, 09670271).

References

Barrett, J.A., Kirschke, H., 1981. cathepsin B, cathepsin H and Cathepsin L. Methods Enzymol. 80, 535–61.

Boulay, C.L., Sellos, D., Wormhoudt, A.V., 1998. Cathepsin L gene organization in crustaceans. Gene 218, 77–84.

Breathnach, R., Chambon, P., 1981. Organization and expression of eukaryotic split genes coding for proteins. Annu. Rev. Biochem. 50, 349–83.

Chapman, C.B., Mitchell, G.F., 1982. Proteolytic cleavage of immunoglobulin by enzymes released by *Fasciola hepatica*. Vet. Parasitol. 11, 165–78.

Chen, M.G., Mott, K.E., 1990. Progress in morbidity due to *Fasciola hepatica* infection. Trop. Dis. Bull. 87, 1–37.

Chomczynski, P., Sacchi, N., 1987. Single-step method of RNA isolation by acid guanidinium thiocyanate-phenol-chloroform extraction. Anal. Biochem. 162, 156–9.

Coulombe, R., Grochulski, R., Sivaraman, J., Menard, R., Mort, J.S., Cygler, M., 1996. Structure of human procathepsin L reveals the molecular basis of inhibition by the prosegment. EMBO J. 15, 5492–503.

Dalton, J.P., Hefferman, M., 1989. Thiol proteases released in vitro by *Fasciola hepatica*. Mol. Biochem. Parasitol. 35, 161–6.

Dalton, J.P., Clough, K.A., Jones, M.K., Brindley, P.J., 1996a. Characterization of the cathepsin-like cysteine proteinases of *Schistosoma mansoni*. Infect. Immun. 64, 1328–34.

Dalton, J.P., McGonigle, S., Rolph, T.P., Andrews, S.J., 1996b. Induction of protective immunity in cattle against infection with *Fasciola hepatica* by vaccination with cathepsin L proteinase and hemoglobin. Infect. Immun. 64, 5066–74.

Davis, E.R., Singh, H., Botka, C., Hardwick, C., el Meanawy, M.A., Villanueva, J., 1994. RNA *trans*-splicing in *Fasciola hepatica*. Identification of a spliced leader (SL) RNA and SL sequences on mRNAs. J. Biol. Chem. 269, 20026–200230.

Day, S.R., Dalton, J.P., Clough, K.A., Leonardo, L., Tiu, W.U., Brindley, P.J., 1995. Characterization and cloning of the cathepsin L proteinases of *Schistosoma japonicum*. Biochem. Biophys. Res. Comm. 217, 1–9.

Dowd, A.J., Smith, M.A., McGonigle, S., Dalton, J.P., 1994. Purification and characterization of a second cathepsin L proteinase secreted by the trematode *Fasciola hepatica*. Eur. J. Biochem. 223, 91–98.

Dowd, A.J., Tort, J., Roche, L., Ryan, T., Dalton, J.P., 1997. Isolation of a cDNA encoding *Fasciola hepatica* cathepsin L2 and functional expression in *Saccharomyces cerevisiae*. Mol. Biochem. Parasitol. 88, 163–74.

Eakin, A.E., Mills, A.A., Harth, G., McKerrow, J.H., Craik, C.S., 1992. The sequence, organization, and expression of the major cysteine protease (cruzain) from *Trypanosoma cruzi*. J. Biol. Chem. 267, 7411–20.

Esteban, J.G., Bargues, M.D., Mas-Coma, S., 1998. Geographical distribution, diagnosis and treatment of human fascioliasis: a review. Res. Rev. Parasitol. 58, 13–48.

Fagbemi, B.O., Guobadia, E.E., 1995. Immunodiagnosis of fascioliasis in ruminants using a 28-kDa cysteine protease of *Fasciola gigantica*. Vet. Parasitol. 57, 309–18.

Fagbemi, B.O., Hillyer, G.V., 1992. Partial purification and characterization of the proteolytic enzymes of *Fasciola gigantica* adult worms. Vet. Parasitol. 40, 217–26.

Grams, R., Vichasri-Grams, S., Sobhom, P., Upatham, E.S., Viyanant, V., 2001. Molecular cloning and characterization of cathepsin L encoding genes from *Fasciola gigantica*. Parasitol. Int. 50, 105–14.

Hashimoto, K., Watanabe, T., Liu, C.X., Init, I., Blair, D., Ohnishi, S., Agatsuma, T., 1997. Mitochondrial DNA and nuclear DNA indicate that the Japanese *Fasciola* species is *F. gigantica*. Parasitol. Res. 83, 220–5.

Hawthorne, S.J., Pagano, M., Halton, D.W., Walker, B., 2000. Partial characterization of a novel cathepsin L-like protease from *Fasciola hepatica*. Biochem. Biophys. Res. Commun. 277, 79–82.

Heussler, T.V., Dobbelaere, A.E.D., 1994. Cloning of a protease gene family of *Fasciola hepatica* by the polymerase chain reaction. Mol. Biochem. Parasitol. 64, 11–23.

Ishidoh, K., Kominami, E., Suzuki, K., Katsunuma, N., 1989. Gene structure and 5′-upstream sequence of rat cathepsin L. FEBS Lett. 259, 71–74.

Karrer, K.M., Peiffer, S.L., DiTomas, M.E., 1993. Two distinct gene subfamilies within the family of cysteine protease genes. Proc. Natl. Acad. Sci. USA 90, 3063–7.

Kreusch, S., Fehn, M., Maubach, G., Nissler, K., Rommerskirch, W., Schilling, K., Weber, E., Wenz, I., Wiederanders, B., 2000. An evolutionarily conserved tripartite tryptophan motif stabilizes the prodomains of cathepsin L-like cysteine proteases. Eur. J. Biochem. 267, 2965–72.

Laemmli, U.K., 1970. Cleavage of structural proteins during the assembly of the head of bacteriophage T4. Nature 227, 680–5.

Liu, D.W., Kato, H., Nakamura, T., Sugane, K., 1996. Molecular cloning and expression of the gene encoding a cysteine proteinase of *Spirometra erinacei*. Mol. Biochem. Parasitol. 76, 11–21.

Maniatis, T., Fritsch, E.F., Sambrook, J., 1982. Molecular Cloning. A Laboratory Manual, Cold Spring Harbor Laboratory, Cold Spring Harbor, NY.

Mas-Coma, S., Esteban, J.G., Bargues, M.D., 1999. Epidemiology of human fascioliasis: a review and proposed new classification. Bull. WHO 77, 340–6.

Matsudaira, P., 1987. Sequence from picomole quantities of proteins electroblotted onto polyvinylidene difluoride membrane. J. Biol. Chem. 262, 10035–8.

Matsumoto, I., Watanabe, H., Abe, K., Arai, S., Emori, Y., 1995. A putative digestive cysteine proteinase from *Drosophila melanogaster* is predominantly expressed in the embryonic and larval midgut. Eur. J. Biochem. 227, 582–7.

Matsumoto, I., Emori, Y., Abe, K., Arai, S., 1997. Characterization of a gene encoding cysteine proteinases of *Sitophilus zeamais* (Maize Weevil), and analysis of the protein distribution in various tissues including alimentary tract and germ cells. J. Biochem. 121, 464–76.

McGinty, A., Moore, M., Halton, D.W., Walker, B., 1993. Characterization of the cysteine proteinase of the common liver fluke *Fasciola hepatica* using novel, active-site directed affinity labels. Parasitology 106, 487–93.

O'Neill, S.M., Parkinson, M., Dowd, A.J., Strauss, W., Angles, R., Dalton, J.P., 1999. Immunodiagnosis of human fascioliasis using recombinant *Fasciola hepatica* cathepsin L1 cysteine proteinase. Am. J. Trop. Med. Hyg. 60, 749–51.

Patthy, L., 1987. Intron-dependent evolution: preferred types of exons and introns. FEBS Lett. 214, 1–7.

Rege, A.A., Herrera, P.R., Lopez, M., Dresden, M.H., 1989. Isolation and characterization of a cysteine proteinase from *Fasciola hepatica* adult worms. Mol. Biochem. Parasitol. 35, 89–95.

Roche, L., Dowd, A.J., Tort, J., McGonigle, S., McSweeney, A., Curley, P., Ryan, T., Dalton, J.P., 1997. Functional expression of *Fasciola hepatica* cathepsin L1 in *Saccharomyces cerevisiae*. Eur. J. Biochem. 245, 373–80.

Roche, L., Tort, J., Dalton, J.P., 1999. The pro-peptide of *Fasciola hepatica* cathepsin L is a potent and selective inhibitor of the mature enzyme. Mol. Biochem. Parasitol. 98, 271–7.

Rosenthal, P.J., Nelson, R.G., 1992. Isolation and characterization of a cysteine proteinase gene of *Plasmodium falciparum*. Mol. Biochem. Parasitol. 51, 143–52.

Saitou, N., Nei, M., 1987. The neighbour-joining method: a new method for reconstructing phylogenetic trees. Mol. Biol. Evol. 4, 406–25.

Smith, A.M., Dowd, A.J., McGonigle, S., Keegan, P.S., Brennan, G., Trudgett, A., Dalton, J.P., 1993. Purification of a cathepsin L-like proteinase secreted by adult *Fasciola hepatica*. Mol. Biochem. Parasitol. 62, 1–8.

Smith, S.M., Gottesman, M.M., 1989. Activity and deletion analysis of recombinant human cathepsin L expressed in *Escherichia coli*. J. Biol. Chem. 264, 20487–95.

Tao, K., Stearns, A.N., Dong, J., Wu, Q.-L., Sahagian, G.G., 1994. The proregion of cathepsin L is required for proper folding, stability, and ER exit. Arch. Biochem. Biophys. 311, 19–27.

Vernet, T., Berti, J.P., Montigny, C., Musil, R., Tessier, C.D., Menard, R., Magny, M.-C., Stoner, C.A., Thomas, Y.D., 1995. Processing of the papain precursor. The ionization state of a conserved amino acid motif within the pro region participates in the regulation of intramolecular processing. J. Biol. Chem. 270, 10838–46.

Wijffels, G.L., Panaccio, M., Salvatore, L., Wilson, L., Walker, I.D., Spithill, T.W., 1994a. The second cathepsin L-like proteinases of the trematode, *Fasciola hepatica*, contain 3-hydroxyproline residues. Biochem. J. 299, 781–90.

Wijffels, G.L., Salvatore, L., Dosen, M., Waddington, J., Thompson, C., Cambell, N., Sexton, J., Wicker, J., Bowen, F., Friedel, T., Spithill, T.W., 1994b. Vaccination of sheep with purified cysteine proteinase of *Fasciola hepatica* decreases worm fecundity. Exp. Parasitol. 78, 132–48.

Yamasaki, H., Aoki, T., Oya, H., 1989. A cysteine proteinase from the liver fluke *Fasciola* spp.: purification, characterization, localization and application to immunodiagnosis. Jpn. J. Parasitol. 38, 373–84.

Yamasaki, H., Kominami, E., Aoki, T., 1992. Immunocytochemical localization of a cysteine protease in adult worms of the liver fluke *Fasciola* sp. Parasitol. Res. 78, 574–80.

Yamasaki, H., Aoki, T., 1993. Cloning and sequence analysis of the major cysteine protease expressed the trematode parasite *Fasciola* sp. Biochem. Mol. Biol. Int. 31, 537–42.

THE JOURNAL OF BIOLOGICAL CHEMISTRY
Vol. 277, No. 32, Issue of August 9, pp. 28934–28941, 2002
Printed in U.S.A.

Ancient Ubiquitous Protein 1 Binds to the Conserved Membrane-proximal Sequence of the Cytoplasmic Tail of the Integrin α Subunits That Plays a Crucial Role in the Inside-out Signaling of $\alpha_{IIb}\beta_3$*

Received for publication, May 3, 2002, and in revised form, May 29, 2002
Published, JBC Papers in Press, May 31, 2002, DOI 10.1074/jbc.M204340200

Atsushi Kato‡§, Norihiko Kawamata‡, Kenji Tamayose‡, Motoki Egashira‡, Rika Miura‡, Tsutomu Fujimura¶, Kimie Murayama¶, and Kazuo Oshimi‡

From the ‡Division of Hematology, Department of Internal Medicine and ¶Division of Biochemical Analysis, Central Laboratory of Medical Sciences, Juntendo University School of Medicine, 2-1-1 Hongo, Bunkyo-ku, Tokyo 113-0033, Japan

Modification of the cytoplasmic tails of the integrin $\alpha_{IIb}\beta_3$ plays an important role in the signal transduction in platelets. We searched for proteins that bind to the α_{IIb} cytoplasmic tail using the yeast two-hybrid assay with a cDNA library of the megakaryocyte-derived cell line and identified a protein, ancient ubiquitous protein 1 (Aup1), that is ubiquitously expressed in human cells. Observation of UT7/TPO cells expressing a red fluorescent protein-tagged Aup1 indicated its localization in the cytoplasm. Immunoprecipitation of UT7/TPO cells by an antibody for Aup1 revealed that ~40% of α_{IIb} is complexed with Aup1. Binding study with an α_{IIb} cytoplasmic tail peptide and glutathione S-transferase-Aup1 fusion protein revealed a low affinity (K_d = 90 μM). Subsequent yeast two-hybrid assay indicated binding of Aup1 to cytoplasmic tails of other integrin α subunits. Binding study with the purified Aup1 and various glutathione S-transferase-α_{IIb} cytoplasmic tail peptides revealed specific binding of Aup1 to the membrane-proximal sequence (KVGFFKR) that is conserved among the integrin α subunits and plays a crucial role in the $\alpha_{IIb}\beta_3$ inside-out signaling. As Aup1 possesses domains related to signal transduction, these results suggest involvement of Aup1 in the integrin signaling.

Integrin $\alpha_{IIb}\beta_3$ (GPIIb-IIIa) is one of the receptors on the cellular surface of platelets and megakaryocytes. It binds to various adhesive proteins including fibrinogen, von Willebrand factor, vitronectin, and fibronectin that contain a core amino acid sequence of arginine-glycine-aspartic acids (RGD). Binding of fibrinogen to $\alpha_{IIb}\beta_3$ leads to platelet aggregation and finally to thrombus formation at the injured vascular sites. A pivotal role of $\alpha_{IIb}\beta_3$ in hemostasis is supported by the clinical observation that the congenital deficiency of $\alpha_{IIb}\beta_3$, Glanzmann's thrombasthenia, results in lifelong bleeding tendency (1). Whereas $\alpha_{IIb}\beta_3$ on resting platelets does not bind soluble fibrinogen, once platelets are activated, conformation of the extracellular domains of the $\alpha_{IIb}\beta_3$ is altered and its ligand-binding affinity is increased (affinity modulation) (2). This process of the inside-out signaling is considered to be mediated by modification of the short cytoplasmic tails of α_{IIb} and β_3 subunits; however, the mechanism remains to be elucidated.

The nuclear magnetic resonance structural analysis of the α_{IIb} cytoplasmic tail revealed a closed conformation where the highly conserved N-terminal membrane-proximal region forms an α-helix followed by a turn, and the acidic C-terminal loop interacts with the N-terminal helix (3). Deletion of almost the entire α_{IIb}-cytoplasmic tail and mutations in its N-terminal sequence (GFFKR) conserved among the integrin α subunits enhance the affinity of $\alpha_{IIb}\beta_3$ for ligands (4–6). The cytoplasmic tail of the β_3 subunit also has an amino acid sequence that is conserved among integrin β subunits: a stretch of 8 amino acids (KLLITIHD) adjacent to the transmembrane domain. In a similar fashion to the α_{IIb} subunit, deletion or mutation in this conserved region induces activation of $\alpha_{IIb}\beta_3$ (6, 7). These observations suggest that membrane-proximal regions of the cytoplasmic domains of both subunits exert a negative regulatory function and lock $\alpha_{IIb}\beta_3$ in a low affinity state. Negative regulation may be mediated by the interaction between α_{IIb} and β_3 cytoplasmic tails, possibly through a salt bridge between Arg-995 in α_{IIb} and Asp-723 in β_3 (6), or binding of intracellular proteins to α_{IIb} and/or β_3 subunits. Two candidates for the modulator proteins have been reported: calcium- and integrin-binding protein (CIB)[1] (8) and β_3-endonexin (9, 10), which bind to α_{IIb} and β_3 cytoplasmic tails, respectively. Although CIB is unlikely to have a regulatory effect on $\alpha_{IIb}\beta_3$ ligand binding function (11), β_3-endonexin fused to GST protein induces the conformational change of $\alpha_{IIb}\beta_3$ and activates it when co-transfected with α_{IIb} and β_3 subunits in Chinese hamster ovary cells. Another mechanism of modification has been recently suggested: an interaction between cytoplasmic tails of $\alpha_{IIb}\beta_3$ and the actin cytoskeleton. $\alpha_{IIb}\beta_3$ and the actin cytoskeleton are physically linked by binding of talin to the β_3 cytoplasmic tail (12), and $\alpha_{IIb}\beta_3$ in resting platelets may be constrained in a low affinity state by the actin cytoskeleton (13). An increase in the cytosolic calcium evoked by agonist stimulation initiates actin filament turnover and may lead to relief of the cytoskeletal

* The costs of publication of this article were defrayed in part by the payment of page charges. This article must therefore be hereby marked "*advertisement*" in accordance with 18 U.S.C. Section 1734 solely to indicate this fact.

§ To whom correspondence should be addressed. Tel.: 81-3-3813-3111; Fax: 81-3-3813-0841; E-mail: atkato@med.juntendo.ac.jp.

[1] The abbreviations used are: CIB, calcium- and integrin-binding protein; Aup1, ancient ubiquitous protein 1; GST, glutathione S-transferase; CUE, coupling of ubiquitin conjugation to the endoplasmic reticulum degradation; PlsC, phosphate acyltransferase; TPO, thrombopoietin; RFP, red fluorescent protein; Tollip, Toll-interacting protein; TAK1, transforming growth factor β-activated kinase 1; TAB2, transforming growth factor β-activated kinase 1-binding protein 2; IL, interleukin; IL-1R, interleukin-1 receptor; IRAK, interleukin-1 receptor-associated kinase; GPAT, glycerophosphate acyltransferase; AGPAT, 1-acylglycerophosphate acyltransferase; LPA, lysophosphatidic acid; PA, phosphatidic acid; FCS, fetal calf serum; PMSF, phenylmethylsulfonyl fluoride; PVDF, polyvinylidene difluoride; MD, membrane-distal; MP, membrane-proximal.

constraints on $\alpha_{IIb}\beta_3$, resulting in a high affinity state of $\alpha_{IIb}\beta_3$. Among these possible modification mechanisms, which one works in platelets remains to be determined.

In contrast, binding of fibrinogen to $\alpha_{IIb}\beta_3$ leads to platelet shape change, release of granules, and platelet aggregation. These sequential biological phenomena are mediated by the outside-in signaling of $\alpha_{IIb}\beta_3$, calcium mobilization, increase in the cytoplasmic pH, thromboxane A_2 generation, and tyrosine phosphorylation of intracellular proteins including focal adhesion kinase and members of the Src family proteins (1). These signaling proteins are complexed with the actin cytoskeleton and are recruited to the focal contacts. In this process, the β_3 cytoplasmic tail (residues 740–762) binds to the adaptor proteins Shc and Grb2 when tyrosine residues (Tyr-747 and Tyr-759) are phosphorylated (14). In addition, the β_3 cytoplasmic tail is involved in clot retraction by transmitting the contractile force evoked by the rearrangement of the cytoskeletal proteins to the extracellular matrix (15). Thus, several proteins that bind to the β_3 cytoplasmic tail and are implicated in the $\alpha_{IIb}\beta_3$ signaling have been identified; however , little is known about proteins that bind to and modify the α_{IIb} cytoplasmic tail.

In this study, we searched for proteins that bind to the α_{IIb} cytoplasmic tail in the thrombopoietin-dependent acute megakaryocytic leukemia-derived cell line, UT7/TPO (16), by the yeast-two hybrid assay and identified a protein, Aup1, that binds to the conserved membrane-proximal sequence of the cytoplasmic tail of the integrin α subunits.

EXPERIMENTAL PROCEDURES

Cell Lines—UT7/TPO cell line (16) was maintained with Iscove's modified Dulbecco's medium supplemented with 20% fetal calf serum (FCS) and 10 ng/ml recombinant human thrombopoietin (TPO) (Kirin Brewery, Tokyo, Japan). Cell lines including HL 60, K562, U937, Jurkat, Raji, and CMK (17), established from acute myelocytic leukemia, chronic myelocytic leukemia, diffuse histiocytic lymphoma, T cell leukemia, Burkitt (B cell) lymphoma, and acute megakaryocytic leukemia, respectively, were maintained with RPMI medium supplemented with 10% FCS. Other cell lines including 293, MCF7, A549, HeLa, and HepG2, established from embryonic kidney, breast carcinoma, lung adenocarcinoma, epitheloid cervical carcinoma, and hepatocarcinoma, respectively, were maintained with Dulbecco's modified Eagle's medium supplemented with 10% FCS.

Amplification of the cDNA Sequence for the Cytoplasmic Domain of Integrin α and β Subunits by PCR—The cDNA sequences for the cytoplasmic domains of various integrin α and β subunits were amplified by reverse transcription-PCR from RNA extracted from UT7/TPO for α_{IIb}, α_2, α_V, and β_3, HepG2 for α_1, Raji for α_5, K562 for α_M, and HL60 for β_1 and β_5, respectively. The cDNA sequences for a mutant α_{IIb} (F992A) and for membrane-proximal (α_{IIb} MP; KVGFFKR) and membrane-distal (α_{IIb} MD; NRPPLEEDDEEGE) segments of the α_{IIb} cytoplasmic tail were amplified using the normal α_{IIb} cytoplasmic tail cDNA. The nucleotide sequence of each cDNA fragment amplified by PCR was confirmed using the ABI Prism dRhodamine terminator cycle sequencing ready reaction kit (Applied Biosystems Japan, Tokyo, Japan).

Yeast Two-hybrid Assays—A cDNA library was constructed by ligating cDNA synthesized from UT7/TPO RNA to a pAD-Gal4 vector (Stratagene, La Jolla, CA). The cDNA sequence for the cytoplasmic domain of the integrin α_{IIb} subunit was ligated in-frame to a pBD-Gal4 vector (Stratagene). Procedures for screening and the filter lift assay to confirm interactions between the bait and target proteins were according to the manufacturer's instructions. Briefly, yeast YRG-2 cells were transformed with a pAD-Gal4 plasmid encoding the UT7/TPO cDNA and a pBD-Gal4 plasmid encoding the α_{IIb} bait. Then, yeast cells were plated on selective SD agar plates without leucine, tryptophan, and histidine (Leu^- Trp^- His^-). Colonies grown on the selective plates, indicating interactions between target and bait proteins, were subjected to the filter lift assay to examine the β-galactosidase activity to confirm the interaction. Positive yeast colonies were transferred to Whatman filter papers, frozen in the liquid nitrogen, thawed, and incubated with 5-bromo-4-chloro-3-indolyl-β-D-galactoside (0.3 mg/ml) in Z buffer (per liter, 16.1 g of $Na_2HPO_4/7H_2O$, 5.5 g of $NaH_2PO_4/7H_2O$, 0.75 g of KCl, 0.246 g of $MgSO_4/7H_2O$, and 2.7 ml of 2-mercaptoethanol; pH 7.0). Colonies that produced blue color were picked up for the subsequent experiments. To examine interactions between the target protein and cytoplasmic tails of various integrin subunits including α_{IIb}, α_1, α_2, α_5, α_M, α_V, β_1, β_2, and β_3, yeast two-hybrid assays were performed in a similar fashion.

Quantitative β-Galactosidase Assay—To compare interactions between the target protein and the cytoplasmic domains of various integrin subunits, the quantitative β-galactosidase assay (18) was performed. Briefly, yeast cells grown in 5 ml of medium at 30 °C until the near log phase (OD_{600} = ~1.0) were resuspended in Z buffer (200 μl) with glycerol (50 μl). After one cycle of freeze-thawing, 1 mM PMSF and acid-washed glass beads were added to the samples, followed by vigorous vortexing. Then, 50 μl of *o*-nitrophenyl-β-D-galactoside (4 mg/ml, Sigma-Aldrich Japan, Tokyo, Japan) was added to the supernatants and the samples were incubated at 30 °C until a yellow color developed. After addition of 120 μl of Na_2CO_3 (1 M), the OD_{420} of each sample was measured. Assays were normalized to the yeast concentration (OD_{600}) of each sample, and the β-galactosidase activity was calculated as follows; β-galactosidase units = $1{,}000 \times OD_{420}/t \times V \times OD_{600}$, where t = time of incubation in minutes, V = volume of culture added to Z buffer in ml (5 ml).

Northern Blot Analysis—Approximately 30 μg of the total RNA extracted from UT7/TPO cells was electrophoresed in 1.5% agarose/formaldehyde gels, transferred to the nylon membranes (Hybond-N+, Amersham Biosciences, Buckinghamshire, United Kingdom), and hybridized with a full-length Aup1 cDNA fragment labeled with [α-^{32}P]dCTP using a random-primed DNA labeling kit (Roche Molecular Biochemicals). To compare the expression of Aup1 transcripts among different human tissues, the Human 12-lane MTN Blot (CLONTECH Japan, Tokyo, Japan) was hybridized with the same probe.

Preparation of the Synthetic Peptides and Antibody Production—Peptides for Aup1 (RLTPADKAEHMKRQRHPRLR) (Fig.1, *A* and *B*), α_{IIb} and β_3 cytoplasmic tails, to which a cysteine residue was added at the N terminus for the antibody production, were synthesized using PSSM-8 (Shimadzu, Kyoto, Japan). Each peptide was coupled to the keyhole limpet hemocyanin (Sigma-Aldrich) and injected subcutaneously to rabbits for immunization.

Immunoblot Analysis—Platelets were isolated from the platelet-rich plasma of the normal peripheral blood, and leukocytes were isolated from the buffy coat after removal of erythrocytes by hypotonic lysis in 0.14 M NH_4Cl, 20 mM Tris (pH 7.2) at 37 °C. Microscopic observation revealed that more than 90% of the prepared leukocytes were neutrophils. To extract proteins, platelets, leukocytes, UT7/TPO, and other cell lines including CMK, HL60, K562, U937, Jurkat, Raji, 293, HepG2, HeLa, MCF7, and A547 were resuspended in the cell lysis buffer (0.15 M NaCl, 10 mM Tris (pH 7.4), 1 mM PMSF, 1.8 μg/ml aprotinin, 100 μg/ml leupeptin, and 1% Triton X-100). Samples were incubated for 30 min on ice with occasional vortexing, and the cell lysates were subjected to 10% SDS-PAGE, transferred to the nitrocellulose membranes (Trans-blot transfer medium, Nippon Bio-Rad Laboratories, Yokohama, Japan). After blocking with 5% skimmed milk in Tris-buffered saline buffer (10 mM Tris (pH 7.4), 150 mM NaCl) for 1 h, membranes were incubated with a preimmune rabbit serum or the rabbit antiserum for the Aup1 peptide (Aup1–2) for 1 h, and then with the horseradish peroxidase-conjugated goat anti-rabbit immunoglobulins (DAKO Japan, Kyoto, Japan). Signals on membranes were detected with the ECL system (Amersham Biosciences).

Subcellular Localization of Aup1—To study the subcellular localization of Aup1, a full-length Aup1 cDNA was ligated into the pDsRed1-N1 vector that encodes a red fluorescent protein (RFP) (CLONTECH). Then, UT7/TPO cells were transfected with a control vector and a plasmid encoding the Aup1-RFP fusion protein by electroporation using the Gene Pulser II (Bio-Rad). After selection with neomycin, stable cell lines that express RFP (UT7/TPO.VR4-4) and Aup1-RFP fusion proteins (UT7/TPO.Aup1 R23-1) were established. To examine the subcellular localization of Aup1, UT7/TPO.VR4-4 and UT7/TPO.Aup1R23-1 cells were applied to glass coverslips and observed using the LSM 510 laser scanning microscope (Carl Zeiss Microscopy, Jena, Germany) with appropriate filters. For the nuclear staining, cells were treated with 3.7% formaldehyde in phosphate-buffered saline and mounted with a medium containing 4′,6′-diamidino-2-phenylindole (Vector Laboratories, Burlingame, CA).

Immunoprecipitation—UT7/TPO cell extracts (600 μg of protein) with the cell lysis buffer containing 1% digitonin and 1 mM Ca^{2+} were incubated with a preimmune rabbit serum or the Aup1–2 antiserum (40 μl) for 1 h, and then with protein-G-Sepharose beads (30 μl) (Amersham Biosciences) for 3 h at 4 °C with gentle shaking. After washing with the

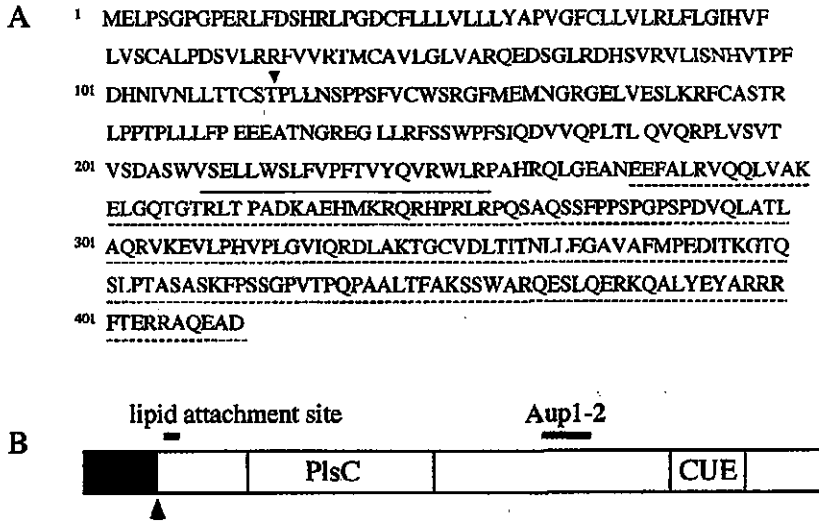

FIG. 1. **Amino acid sequence and a schematic representation of Aup1.** *A*, the *arrowhead* indicates the position where 66 amino acids are inserted in the reported long isoform (Ref. 21; GenBank™ accession no. AF100754). The *solid line* indicates the amino acid sequence, against which the rabbit antiserum (Aup1–2) was raised. The *broken line* indicates the sequence encoded by 48L21 that was identified by the yeast two-hybrid assay. *B*, the *shaded area* and the *arrowhead* represent a putative signal sequence and a signal cleavage site, respectively. *Aup1–2*, the peptide used for antibody production; *PlsC*, phosphate acyltransferase domain; *CUE*, coupling of ubiquitin conjugation to the endoplasmic reticulum degradation domain.

cell lysis buffer, the beads were resuspended in the SDS sample buffer and boiled, and the supernatants were subjected to SDS-PAGE, followed by immunoblot analysis using mouse monoclonal antibodies for the α_{IIb} (SZ22, Cosmo Bio, Tokyo, Japan) and β_3 subunits (SZ21, Cosmo Bio). Signals were detected with the ECL system after incubation with the horseradish peroxidase-conjugated rabbit anti-mouse immunoglobulins (DAKO). To measure how much part of the cellular α_{IIb} is complexed with Aup1, the immunodepletion assay was performed. After preincubation with protein-G beads, UT7-TPO cell lysates (500 μg of protein) were immunoprecipitated twice with the control rabbit or the Aup1–2 serum (40 μl) and protein-G beads (50 μl). Then, aliquots of the supernatants (1–10 μl) were subjected to SDS-PAGE, followed by immunoblot analysis using the polyvinylidene difluoride (PVDF) membrane (Immobilon-P, Millipore, Bedford, MA) and the SZ22 antibody. Concentration of the residual (free) α_{IIb} subunit was quantified by densitometry of the respective α_{IIb} bands to calculate the percentage of α_{IIb} bound to Aup1.

GST Pull-down Assay—The cDNA sequences for Aup1, the normal and a mutant (F992A) α_{IIb} cytoplasmic tails, and the membrane-proximal (α_{IIb} MP) and membrane-distal segments (α_{IIb} MD) were ligated in-frame to the pGEX-4T vector that encodes GST (Amersham Biosciences). For production of GST fusion proteins, DH5α cells transfected with the respective plasmids were incubated at 25 °C until the culture reached the mid-log phase (OD_{600} = ~0.8), at which time 25 μM isopropyl-β-D-thiogalactopyranoside was added. After incubation for an additional 2 h, the bacteria were resuspended in phosphate-buffered saline containing 1 mM PMSF and 1 mg/ml lysozyme, followed by sonication. Triton X-100 was then added (1%), and the supernatant was incubated with the GSH-Sepharose beads (Amersham Biosciences) for 30 min at room temperature, followed by washing with phosphate-buffered saline. To examine association between Aup1 and cytoplasmic tails of α_{IIb} and β_3, beads that bound the GST-Aup1 fusion protein (125 μg) and the control GST protein (62.5 μg) were incubated with the UT7/TPO cell extract (1 mg of protein) in the GST reaction buffer (200 μl, the cell lysis buffer containing 1% Triton X-100) for 3 h at 4 °C with gentle shaking. Thereafter, beads were washed with the GST reaction buffer, resuspended in the SDS sample buffer, and boiled, and the supernatant was subjected to SDS-PAGE, followed by immunoblot analysis using the PVDF membrane, the rabbit antiserum for the cytoplasmic tails of α_{IIb} and β_3, and the horseradish peroxidase-conjugated goat anti-rabbit immunoglobulins. To identify the α_{IIb} sequence to which Aup1 binds, Aup1 cleaved from the immobilized GST-Aup1 fusion protein by thrombin (Sigma-Aldrich) according to the manufacturer's instructions was preincubated with GSH- and GST-Sepharose beads in the GST reaction buffer. Then, the supernatants (50 μl containing 0.7 μg of Aup1; 0.4 μM) was incubated with the immobilized GST-α_{IIb} cytoplasmic tail fusion proteins (20 μM), including the normal and a mutant (F992A) α_{IIb}, α_{IIb} MP, and α_{IIb} MD segments, followed by SDS-PAGE and immunoblot analysis using the PVDF membrane and the Aup1–2 antiserum.

Estimation of the Affinity of Interaction between Aup1 and the α_{IIb} Cytoplasmic Tail—The synthetic α_{IIb} cytoplasmic peptide was preincubated with the GST-Sepharose beads for 30 min at room temperature, and the supernatants (20–720 μM) were incubated with the immobilized GST-Aup1 fusion protein (1 μg, 1.5 μM) for 1 h at room temperature in the GST reaction buffer (10 μl). Then, various amounts of the supernatants, the original α_{IIb} peptide, and the peptide preabsorbed by GST beads were subjected to 15% SDS-PAGE, followed by immunoblot analysis using the PVDF membrane and the rabbit antiserum for the α_{IIb} cytoplasmic tail. The resulting immunoblots of the α_{IIb} cytoplasmic tail were quantified by densitometry, and the affinity of Aup1 for binding to the α_{IIb} cytoplasmic tail was calculated by Scatchard analysis (19).

RESULTS

Identification of a Protein That Binds to the Integrin α_{IIb} Cytoplasmic Tail—To search for proteins that bind to the cytoplasmic tail of the integrin α_{IIb} subunit, we constructed a cDNA library from a megakaryocyte-derived cell line, UT7/TPO. UT7/TPO cells constitutively express $\alpha_{IIb}\beta_3$ on the cellular surface, as confirmed by fluorescence-activated cell sorting analysis (data not shown). Screening of the cDNA library by the yeast two-hybrid assay with a bait of the α_{IIb} cytoplasmic tail identified a 900-bp cDNA fragment that encodes a partial C-terminal peptide composed of 173 amino acids (48L21) (Fig. 1*A*). To obtain a cDNA sequence for the N-terminal portion, we performed PCR using UT7/TPO cDNA and primers from the 5′-terminal sequence of the cloning site of pAD-Gal4 (5′-AGGGATGTTTAATACCACTAC-3′) and the 5′-terminal sequence of the 48L21 (5′-GCTGTTGTACACGGAGTGCA-3′). A 400-bp cDNA fragment (5′-48L21) was amplified, and the nucleotide sequencing revealed the sequence was continuous to the 5′-terminus of 48L21. For the final cloning of a full-length cDNA, PCR with UT7/TPO cDNA and primers from the 5′-terminal sequence of 5′-48L21 (5′-TGCGCCTGGGCGCGAAAATG-3′) and 3′-terminal sequence of 48L21 (5′-GGCTCTGGGTGCCATCCTGT-3′) was performed. Nucleotide sequencing of the amplified PCR product (1.3-kb cDNA fragment) revealed that the protein was composed of 410 amino acids. Subsequent data

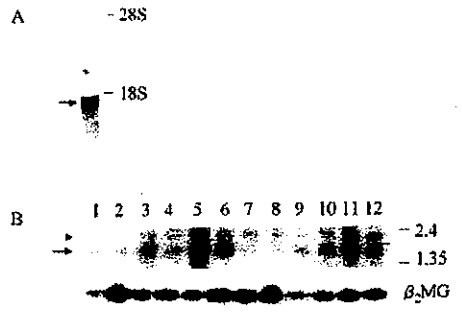

FIG. 2. **Expression of the Aup1 transcripts in human cells and tissues.** *A*, total RNA of UT7/TPO cells was probed with a ^{32}P-labeled Aup1 cDNA fragment. *B*, mRNA on the Human 12-lane MTN Blot (CLONTECH) was hybridized with the same probe; leukocytes (*lane 1*), lung (*lane 2*), placenta (*lane 3*), small intestine (*lane 4*), liver (*lane 5*), kidney (*lane 6*), spleen (*lane 7*), thymus (*lane 8*), colon (*lane 9*), skeletal muscle (*lane 10*), heart (*lane 11*), and brain (*lane 12*). *Arrows* indicate an Aup1 transcript (~1.7 kb), and the *arrowhead* (~2.1 kb) (B) may represent an alternatively spliced transcript. Molecular size markers are presented (28 and 18 S; ribosomal RNA, 2.4 and 1.35 (RNA size markers in kb)). *β_2MG*, filters were reprobed with a ^{32}P-labeled β_2-microglobulin cDNA.

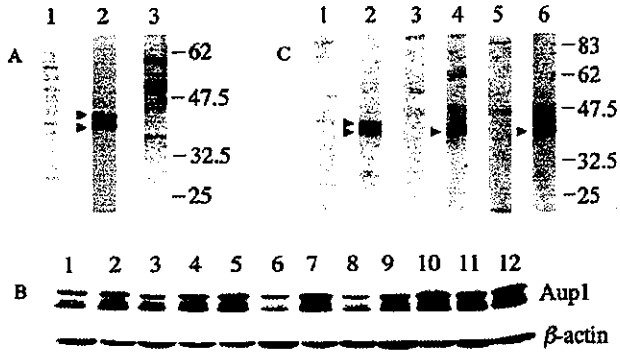

FIG. 3. **Expression of Aup1 protein in human cells.** *A*, protein (150 μg) extracted from UT7/TPO cells were probed with a preimmune rabbit serum (*lane 1*), a rabbit antiserum for Aup1 (Aup1–2) (*lane 2*), and Aup1–2 with a synthetic Aup1 peptide (80 nM) (*lane 3*). Duplicate bands disappeared when an Aup1 peptide was added to the Aup1–2 antiserum, indicating that Aup1–2 recognizes the peptide sequence (*lane 3*). Protein size markers (kDa) are presented. *B*, protein extracts (150 μg) from human cell lines including 293 (*lane 1*), MCF7 (*lane 2*), A549 (*lane 3*), HeLa (*lane 4*), HepG2 (*lane 5*), Jurkat (*lane 6*), Raji (*lane 7*), U937 (*lane 8*), K562 (*lane 9*), HL 60 (*lane 10*), CMK (*lane 11*), and UT7/TPO (*lane 12*) were probed with Aup1–2. β-actin; filters were reprobed with an anti-β actin antibody (Sigma). *C*, protein extracts from UT7/TPO cells (150 μg, *lanes 1* and *2*), platelets (100 μg, *lanes 3* and *4*), and leukocytes (125 μg, *lanes 5* and *6*) were probed with a preimmune rabbit serum (*lanes 1*, *3*, and *5*) and Aup1–2 (*lanes 2*, *4*, and *6*). *Arrowheads* indicate Aup1. Although duplicate bands of ~40 kDa were observed in cell lines, only a smaller band was detected in platelets and leukocytes.

base searches indicated that the sequence was identical with the short isoform of Aup1 (Refs. 20 and 21; GenBank™ accession no. AF100753) (Fig. 1, *A* and *B*).

Aup1 Is Ubiquitously Expressed in Human Cells and Tissues—Northern blot analysis with the total RNA extracted from UT7/TPO cells using a full-length Aup1 cDNA probe revealed a transcript of ~1.7 kb (Fig. 2*A*). Because it was reported that Aup1 is expressed in all mouse tissues (20), we examined the expression of Aup1 transcripts in various human tissues. In concordance with the mouse tissues, Aup1 was expressed in all human tissues examined (Fig. 2*B*). To examine the expression of the Aup1 protein in UT7-TPO cells, platelets, leukocytes, and other cell lines, a rabbit antiserum was raised against a synthetic peptide for Aup1 (Fig. 1, *A* and *B*). Immunoblot analysis using this antiserum (Aup1–2) revealed duplicate bands of ~40 kDa at the reducing as well as non-reducing conditions in UT7/TPO cells (Fig. 3*A*). These bands were observed in other cell lines including CMK, HL60, K562, U937, Jurkat, Raji, HepG2, 293, HeLa, MCF7, and A547 (Fig. 3*B*). Treatment with the protein phosphatases did not change intensity of these two bands (data not shown). In contrast, only a smaller band was detected in platelets and leukocytes (Fig. 3*C*).

Aup1 Is Present in Cytoplasm—To examine the subcellular localization of Aup1, stable UT7/TPO cell lines that express the Aup1-RFP fusion protein (UT7/TPO.Aup1R23-1) and the control RFP (UT7/TPO.VR4-4) were established. Overexpression of Aup1 did not affect the expression of $\alpha_{IIb}\beta_3$ on the cellular surface, as confirmed by fluorescence-activated cell sorting analysis of UT7/TPO, UT7/TPO.VR4-4, and UT7/TPO.Aup1R23-1 cells (data not shown). Observation of UT7/TPO.VR4-4 and UT7/TPO.Aup1 R23-1 cells by confocal microscopy revealed that RFP was distributed evenly throughout the cell; however, the Aup1-RFP fusion protein was observed in the cytoplasm, but not in the nucleus (Fig. 4). Because it was reported that the N terminus of mouse Aup1 resembles the signal peptide of secreted protein, followed by a putative signal cleavage site, we examined whether Aup1 is secreted from cells. Immunoblot analysis with the culture supernatant of UT7/TPO cells using the Aup1–2 antiserum revealed that Aup1 could not be detected in the concentrated (10-fold) culture supernatant (data not shown). These results indicate that Aup1 is a cytoplasmic protein.

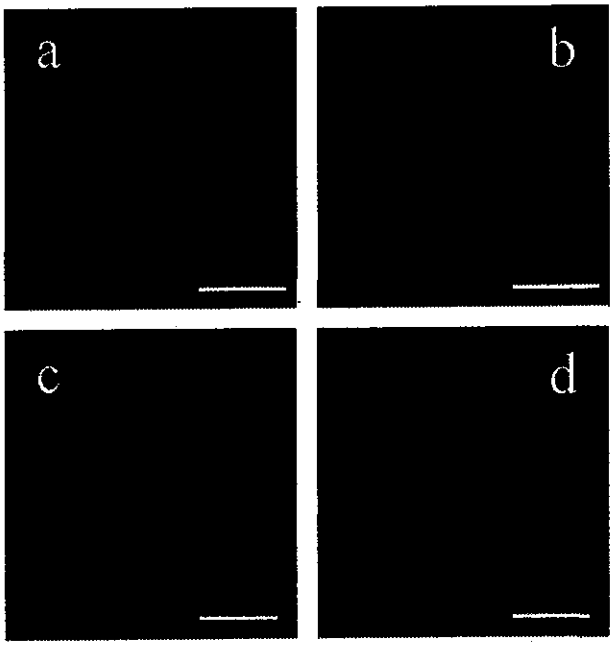

FIG. 4. **Subcellular localization of Aup1.** Confocal microscopy of the stable UT7/TPO cell lines expressing an RFP (UT7/TPO.VR4-4) (*a* and *c*) and an Aup1-RFP fusion protein (UT7/TPO.Aup1R23-1) (*b* and *d*). Nucleus was stained by 4′,6′-diamidino-2-phenylindole (*c* and *d*). Although RFP is distributed evenly throughout the cell (*a* and *c*), the Aup1-RFP fusion protein was observed in the cytoplasm without localization in the nucleus (*b* and *d*). *White bars* represent 10 μm.

Approximately 40% of the α_{IIb} Subunit Is Complexed with Aup1 in UT7/TPO Cells—To examine whether Aup1 is associated with the α_{IIb} cytoplasmic tail in the eukaryotic cells, UT7-TPO cell lysate was immunoprecipitated with the Aup1–2 antiserum. Immunoblot analysis with the precipitates using anti-α_{IIb} and -β_3 antibodies indicated that Aup1 bound to the

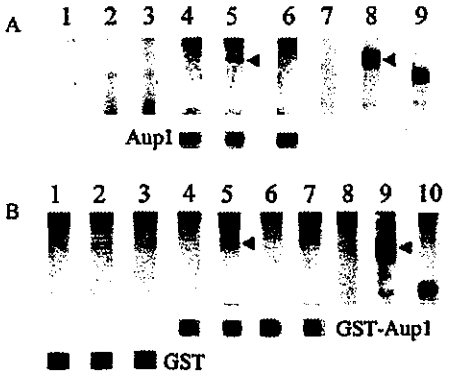

FIG. 5. **Interaction between Aup1 and the cytoplasmic tail of the integrin α_{IIb} subunit.** *A*, immunoprecipitation. UT7/TPO cell lysate (600 μg of protein) coprecipitated with a preimmune rabbit serum (*lanes 1–3*) and an antiserum for Aup1 (Aup1–2) (*lanes 4–6*), and the control lysate (30 μg, *lanes 7–9*) were probed with the control mouse immunoglobulin (*lanes 1, 4,* and *7*), the mouse monoclonal antibodies for α_{IIb} (SZ22) (*lanes 2, 5,* and *8*) and β_3 (SZ21) subunits (*lanes 3, 6,* and *9*). *Arrowheads* indicate the α_{IIb} subunit. Filters (*lanes 4–6*) were reprobed with the antiserum for Aup1 (Aup1–2) (*strips below lanes 4–6*). *B*, GST pull-down assay. Control GST protein (*lanes 1–3*) and the GST-Aup1 fusion protein (*lanes 4–7*) that bound to GSH-Sepharose beads were incubated with UT7/TPO cell lysates. These samples (*lanes 1–7*) and the UT7/TPO cell lysate (100 μg of protein, *lanes 8–10*) were probed with a preimmune rabbit serum (*lanes 1, 4,* and *8*), rabbit antiserum against α_{IIb} (*lanes 2, 5,* and *9*) and β_3 cytoplasmic tails (*lanes 3, 7,* and *10*). To examine competition, the α_{IIb} cytoplasmic tail peptide (0.8 μM) was added to the antiserum against the same peptide (*lane 6*). *Arrowheads* indicate α_{IIb} subunits. Strips were reprobed with the goat antiserum for GST (Amersham Biosciences); GST (*strips below lanes 1–3*) and GST-Aup1 fusion protein (*strips below lanes 4–7*).

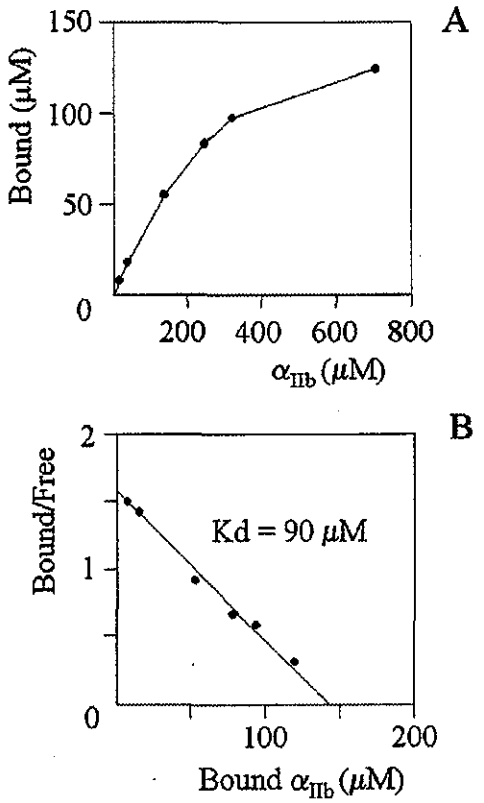

FIG. 6. **Estimation of the affinity of interaction between Aup1 and the α_{IIb} cytoplasmic tail.** *A*, various amounts of the synthetic peptide for the α_{IIb} cytoplasmic tail were incubated with the immobilized GST-Aup1 fusion protein, followed by SDS-PAGE and immunoblot analysis with the antiserum for the α_{IIb} cytoplasmic tail. The amounts of the α_{IIb} peptide bound to Aup1 were quantified by densitometry. *B*, Scatchard plot of the same data was linear, giving K_d value of 90 μM.

α_{IIb}, but not to the β_3 subunit (Fig. 5*A*). We then measured how much of the cellular α_{IIb} subunit is complexed with Aup1 by the immunodepletion assay. Densitometric analysis of the resulting α_{IIb} bands with the supernatants of the UT7-TPO cell lysate after immunoprecipitation with the Aup1–2 and the control rabbit serum revealed that 41.7 ± 3.2% (mean ± S.D., results from three independent experiments) of the α_{IIb} subunit was complexed with Aup1 (data not shown). Binding of Aup1 to the α_{IIb} cytoplasmic tail was confirmed by the GST pull-down assay, revealing that GST-tagged Aup1 binds to the α_{IIb}, but not to the β_3 subunit (Fig. 5*B*).

Aup1 Interacts with the α_{IIb} Cytoplasmic Tail with a Low Affinity—We next studied interaction between the synthetic peptide for the α_{IIb} cytoplasmic tail and immobilized GST-Aup1 fusion protein to measure the affinity of interaction. The K_d value calculated from the Scatchard plot analysis was 90 μM, suggesting a relatively weak affinity of interaction between Aup1 and the α_{IIb} cytoplasmic tail (Fig. 6).

Aup1 Binds to Cytoplasmic Tails of Various Integrin α Subunits—As Aup1 is expressed ubiquitously in human cells and tissues, we examined whether Aup1 binds to cytoplasmic tails of other integrin α as well as β subunits by the yeast two-hybrid assays. Yeast cells were co-transformed with plasmids encoding Aup1 (48L21) and cytoplasmic tails of α_{IIb}, α_1, α_2, α_5, α_V, α_M, β_1, β_2, and β_3. In selective Leu$^-$ Trp$^-$ His$^-$ plates, only colonies co-transformed with Aup1 and α subunits grew. These colonies were positive for both of the filter lift assay and the quantitative β-galactosidase assay (Fig. 7). These results indicate that Aup1 binds to cytoplasmic tails of various integrin α subunits.

Aup1 Binds to the Conserved Membrane-proximal Sequence of the Cytoplasmic Tail of the Integrin α Subunits—The amino acid sequence of the membrane-proximal region of the cytoplasmic tail is highly conserved among the integrin α subunits and plays a crucial role in the inside-out signaling of $\alpha_{IIb}\beta_3$ (4–6).

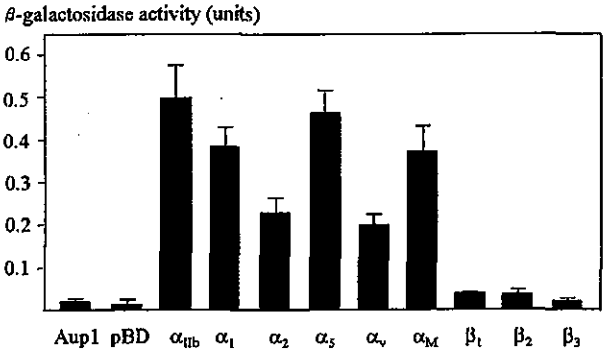

FIG. 7. **Quantitative β-galactosidase assay indicating associations between Aup1 and cytoplasmic tails of the integrin α subunits.** Interactions between Aup1 and cytoplasmic tails of various integrin α and β subunits in the yeast two-hybrid assay are presented as activity of β-galactosidase. Yeast cells transfected with Aup1 (Aup1), Aup1 with the control pBD-Gal4 vector (pBD), Aup1 with α subunits (α_{IIb}, α_1, α_2, α_5, α_V, and α_M), and Aup1 with β subunits (β_1, β_2, and β_3), were grown in Leu$^-$, Leu$^-$ Trp$^-$, Leu$^-$ Trp$^-$ His$^-$, and Leu$^-$ Trp$^-$ selective medium, respectively. *Bars* represent the mean ± S.D. of three separate experiments, each performed on five independent colonies.

As the results from the yeast two-hybrid assay suggested binding of Aup1 to this conserved sequence, we examined interaction between the purified Aup1 and immobilized GST fusion proteins of the α_{IIb} cytoplasmic tail, including the normal and a mutant (F992A) α_{IIb} that leads to the high affinity state of

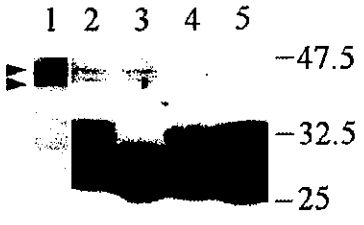

FIG. 8. **Interaction between Aup1 and GST-α_{IIb} cytoplasmic tail fusion proteins.** 50 ng of the purified Aup1 (*lane 1*) and 0.7 μg (0.4 μM) incubated with the immobilized GST fusion proteins (20 μM) of the α_{IIb} cytoplasmic tail, including the normal α_{IIb} (*lane 2*), membrane-proximal sequence (KVGFFKR) (*lane 3*), membrane-distal sequence (NRPPLEEDDEEGE) (*lane 4*), and a mutant α_{IIb} (F992A) (*lane 5*), were subjected to immunoblot analysis using antiserum for Aup1 (Aup1–2). *Arrowheads* represent Aup1 and *thick bands* at the *bottom* of *lanes 2–5* represent respective GST-α_{IIb} cytoplasmic peptide fusion proteins.

$\alpha_{IIb}\beta_3$ (6), and the membrane-proximal (KVGFFKR) and membrane-distal (NRPPLEEDDEEGE) sequences. The GST pull-down assay revealed binding of Aup1 to the normal and the membrane-proximal α_{IIb} sequence, but neither to the mutant nor to the membrane-distal sequence (Fig. 8). These results indicate that Aup1 binds to the specific short amino acid stretch that is located at the membrane-proximal region and conserved among the cytoplasmic tails of the integrin α subunits.

DISCUSSION

One of the obstacles to elucidate the integrin $\alpha_{IIb}\beta_3$ signaling is the absence of appropriate cell lines that exhibit similar properties to platelets including expression of $\alpha_{IIb}\beta_3$ and intracellular signaling molecules, and the response to platelet physiological agonists. Because the α_{IIb} subunit is exclusively expressed in platelets and megakaryocytes, it is suggested that a megakaryocyte-derived cell line would be suitable to search for proteins that bind to the α_{IIb} cytoplasmic tail. In this study, we performed the yeast two-hybrid assay and screened the cDNA library from UT7/TPO cells using the α_{IIb} cytoplasmic tail as bait. Binding of Aup1 to the α_{IIb} cytoplasmic tail was demonstrated by the following results. First, Aup1 bound to the α_{IIb} cytoplasmic tail in the yeast two-hybrid assay. Second, Aup1 is a cytoplasmic protein, as indicated by the observation with the confocal microscopy of UT7/TPO cells that express an RFP-tagged Aup1. Third, the α_{IIb} subunit was present in the immunoprecipitate of the UT7-TPO cell lysate by the antiserum for Aup1. Fourth, GST-tagged Aup1 bound to the α_{IIb} subunit in the UT7-TPO cells.

The N terminus of Aup1 is hydrophobic and resembles the signal sequence of secreted proteins, followed by an 11-amino acid sequence with similarity to a prokaryotic lipid attachment site (20) (Fig. 1*B*). These characteristic amino acid sequences and the present observations with confocal microscopy and immunoblot analysis with the culture supernatant of UT7/TPO cells suggest that Aup1 is a cytoplasmic protein in possible association with the plasma membrane. Immunoblot analysis with the antiserum for an Aup1 peptide revealed duplicate bands of ~40 kDa with an estimated molecular mass difference of ~3–4 kDa in UT7/TPO and other cell lines. In contrast, only a smaller band was detected in platelets and leukocytes. Although only a single cDNA fragment encoding 410 amino acids was amplified by PCR with UT7/TPO cDNA in the present study, a long isoform of Aup1 composed of 476 amino acids has been reported to be produced by alternative splicing of the Aup1 gene (21). However, considering the difference in the number of amino acids (66) between these two isoforms, it is unlikely that duplicate bands observed in the immunoblot analysis are produced by alternative splicing. Another possible examination is the posttranslational modification including glycosylation, phosphorylation, and cleavage. As the consensus amino acid sequences for the *O*- and *N*-linked glycosylation sites are absent in Aup1 and only a smaller band is observed in terminally differentiated platelets and leukocytes, it is hard to explain that the larger protein represents a glycosylated mature protein. With regard to phosphorylation, tyrosine, serine, and/or threonine residues are phosphorylated upon cellular stimulation as observed in a number of intracellular signaling proteins. However, modification by phosphorylation is unlikely because duplicate bands were constitutively expressed and did not exhibit any difference in their intensity after treatment with the protein phosphatase in the immunoblot analysis. On the other hand, the difference in the estimated molecular mass of these two bands (~3–4 kDa) is concordant with that of the postulated signal sequence composed of 37 amino acids. Accordingly, it is conceivable that a larger band represents a precursor protein subjected to cleavage to the smaller mature protein, followed by possible modification with lipid attachment including myristoylation, prenylation, and/or palmitoylation to be associated with the internal leaflet of the plasma membrane (22).

It was reported that mouse Aup1 also consists of 410 amino acids and is expressed in all mouse tissues. In addition, it exhibits an amino acid sequence similar to those of *Caenorhabditis elegans* and human Aup1 (20). Because of its evolutionary conservation of the amino acid sequence and ubiquitous expression, it appears that Aup1 plays an essential role in cell biology. It was unexpected that Aup1, a ubiquitously expressed protein in various tissues, binds to the cytoplasmic tail of the α_{IIb} subunit that is exclusively expressed in platelets and megakaryocytes. Accordingly, we examined whether Aup1 binds to the cytoplasmic tails of other integrin α as well as β subunits. The yeast two-hybrid assays revealed that Aup1 binds to the cytoplasmic tails of the α_1, α_2, α_5, α_M, and α_V subunits, but not to the β_1, β_2, and β_3 subunits, indicating specific binding of Aup1 to the integrin α subunits. To confirm association between Aup1 and these α subunits, we performed immunoprecipitation using cell lines that express a relatively high level of these α subunits, including IMR32 treated by retinoic acid for α_1, CCRF-CEM for α_2, HeLa treated by IL-6 for α_5, K562 for α_M, and RAW264.7 for α_V. However, we could co-precipitate Aup1 with these integrin α subunits neither by the Aup1–2 nor by various antiserum for these subunits, probably because the expression level of these proteins is extremely low compared with the α_{IIb} subunit in UT7/TPO cells (data not shown). On the other hand, subsequent GST pull-down assay indicated binding of Aup1 to the membrane-proximal amino acid sequence (KVGFFKR) that is conserved among the cytoplasmic tails of the integrin α subunits. Accordingly, it seems that one of the essential biological functions of Aup1 is to bind to the cytoplasmic tail of the integrin α subunits through the conserved membrane-proximal sequence.

A data base search for the homologous domain structure revealed that Aup1 possesses two domains: CUE and PlsC domains (23). The yeast protein Cue1p is a prototype of CUE domain family and belongs to the integral endoplasmic reticulum membrane proteins. It exhibits a scaffolding activity and recruits the ubiquitin-conjugating enzymes Ubc7p and Ubc6p in the proximity of the translocon pore cytoplasmic exit to deliver proteins for ubiquitination and subsequent digestion by the proteasome (24). The CUE domain is also present in several eukaryotic cytoplasmic proteins. It was suggested that some of the CUE-containing proteins are not associated with endoplasmic reticulum and possess functions different from that of Cue1p (23). Recent studies identified two eukaryote proteins with the CUE domain, Toll-

interacting protein (Tollip) and transforming growth factor β-activated kinase1 (TAK1)-binding protein 2 (TAB2), that exhibit novel functions in the IL-1 signal transduction pathway. Tollip is present in a complex with the serine/threonine IL-1 receptor (IL-1R)-associated kinase (IRAK) and binding of IL-1 to IL-1R results in the rapid assembly of a membrane-proximal signaling complex that consists of IL-1R, an adaptor protein (myeloid differentiation protein; MyD88), IRAK, and Tollip. Because overexpression of Tollip results in impaired IL-1β-induced activation of the nuclear transcription factor κB and c-Jun N-terminal kinase, it may inhibit IL-1 signaling by silencing components of the signaling cascade including IRAK (25). TAB2 is an adaptor protein that mediates activation of TAK1. IL-1 stimulates translocation of TAB2 from the membrane to the cytosol where it mediates association of TAK1 with the tumor necrosis factor receptor-associated factor 6 (TRAF6), leading to activation of TAK1 (26).

In addition to possessing the CUE domain, the amino acid sequence of Aup1 exhibits a significant similarity to taffazins that belong to the acyltransferase superfamily (27, 28), suggesting that Aup1 may exhibit an enzymatic activity. Taffazins are composed of a highly hydrophobic N terminus of 30 amino acids that may serve a membrane anchor and a central hydrophilic domain composed of 72 residues that may serve as an exposed loop interacting with other proteins. Mutations of a gene encoding taffazins (G4.5) lead to a severe inherited (X-linked) disorder, Barth syndrome, that is characterized by cardiac and skeletal myopathy, short stature, and neutropenia, indicating an essential biological function of taffazins (29). Acyltransferases of the tafazzin superfamily all function in phospholipid synthesis and have either glycerophosphate (GPAT, EC 2.3.15), 1-acylglycerophosphate (AGPAT, EC2.3.1.51), 2-acylglycerophosphate, or 2-acylglycerophosphoethanolamine acyltransferase activity (28). The initial step of phospholipid biosynthesis involves the acylation of glycerol-3-phosphate by GPAT to form lysophosphatidic acid (LPA), followed by acylation of LPA by AGPAT to form phosphatidic acid (PA). In addition to being the key intermediates in the phospholipid biosynthesis, PA and LPA are the essential lipid messengers in signal transduction. Thrombin stimulation leads to production of LPA, followed by its extracellular release in platelets. Binding of LPA to its G protein-coupled receptor leads to stimulation of phospholipases C and D, inhibition of adenylyl cyclase, activation of Ras and the downstream Raf/mitogen-activated protein kinase pathway, and tyrosine phosphorylation of focal adhesion proteins accompanied by remodeling of the actin cytoskeleton in the integrin signaling pathway (30). In contrast, PA can act as an intracellular as well as an extracellular messenger, activating phospholipase C and the numerous protein kinases involved in the signal transduction of the protein kinase C and Raf/mitogen-activated protein kinase pathways (31, 32). Moreover, fibrinogen binding to $\alpha_{IIb}\beta_3$ incorporated into PA-containing lipid vesicles is enhanced, indicating that PA can modulate affinity of $\alpha_{IIb}\beta_3$ within a membrane environment (33). Implications in signal transduction have also been reported both with GPAT and AGPAT; insulin and epidermal growth factor activate GPAT and increase *de novo* PA synthesis, which may amplify diacylglycerol-protein kinase C signaling (34). Stimulation with IL-1β increases AGPAT activity and leads to an enhanced transcription and synthesis of tumor necrosis factor-α and IL-6, suggesting AGPAT may amplify cellular signaling responses from cytokines (32).

Taken together, it is conceivable that Aup1 is involved in the integrin signaling. Binding of Aup1 to the cytoplasmic tail of the integrin α subunits may alter interactions between α and β cytoplasmic tails, including interference of the salt bridge formation as predicted between Arg-995 in α_{IIb} and Asp-723 in β_3. Otherwise, Aup1 may function as an adaptor protein by its CUE domain and recruit signaling molecules to integrin cytoplasmic tails, or exert a phosphate acyltransferase activity by its PlsC domain, leading to alternation in the local concentrations of PA and LPA. Consequently, conformation of the integrin extracellular domains may be altered (inside-out signaling), or the sequential biological phenomenon evoked by ligand binding may be modulated (outside-in signaling). The GST pull-down assay indicated binding of Aup1 to the conserved membrane-proximal sequence of the integrin α subunits. As deletions or mutations in this region lead to an increase in the affinity of $\alpha_{IIb}\beta_3$ for ligands (4–6) and a mutation in this region (F992A) prevents binding of Aup1, it is conceivable that binding of Aup1 to this sequence may sustain integrin in a low affinity state. In the inside-out signaling of platelets, thrombin stimulation leads to the rapid activation of tyrosine kinases, including Syk, which is activated within seconds (35), and Src family kinases, and tyrosine phosphorylation of the signaling proteins (36). Considering the remarkable rapidity of this signaling process, Aup1 which binds to the α_{IIb} cytoplasmic tail reversibly as suggested by the relatively low affinity of interaction, may be suitable for one of the modulators in the $\alpha_{IIb}\beta_3$ inside-out signaling. However, further studies are necessary to elucidate implication of Aup1 in the integrin signaling and other biological functions.

Acknowledgment—We are grateful to Dr. N. Komatsu for providing UT7/TPO cells.

REFERENCES

1. Kato, A. (1997) *Crit. Rev. Oncol./Hematol.* **26,** 1–23
2. Smyth, S. S., Joneckis, C. C., and Parise, L. V. (1993) *Blood* **81,** 2827–2843
3. Vinogradova, O., Haas, T., Plow, E. F., and Qin, J. (2000) *Proc. Natl. Acad. Sci. U. S. A.* **97,** 1450–1455
4. O'Toole, T. E., Mandelman, D., Forsyth, J., Shattil, S. J., Plow, E. F., and Ginsberg, M. H. (1991) *Science* **254,** 845–847
5. O'Toole, T. E., Katagiri, Y., Faull, R. J., Peter, K., Tamura, R., Quaranta, V., Loftus, J. C., Shattil, S. J., and Ginsberg, M. H. (1994) *J. Cell Biol.* **124,** 1047–1059
6. Hughes, P. E., Diaz-Gonzalez, F., Leong, L., Wu, C., McDonald, J. A., Shattil, S. J., and Ginsberg, M. H. (1996) *J. Biol. Chem.* **271,** 6571–6574
7. Hughes, P. E., O'Toole, T. E., Ylanne, J., Shattil, S. J., and Ginsberg, M. H. (1995) *J. Biol. Chem.* **270,** 12411–12417
8. Naik, U. P., Patel, P. M., and Paraise, L. V. (1997) *J. Biol. Chem.* **272,** 4651–4654
9. Shattil, S. J., O'Toole, T., Eigenthaler, M., Thon, V., Williams, M., Babior, B. M., and Ginsberg, M. H. (1995) *J. Cell Biol.* **131,** 807–816
10. Kashiwagi, H., Schwartz, M. A., Eigenthaler, M., Davis, K. A., Ginsberg, M. H., and Shattil, S. J. (1997) *J. Cell Biol.* **137,** 1433–1443
11. Vallar, L., Melchior, C., Plançon, S., Drobecq, H., Lippens, G., Regnault, V., and Kieffer, N. (1999) *J. Biol. Chem.* **274,** 17257–17266
12. Calderwood, D. A., Zent, R., Grant, R., Rees, D. J., Hynes, R. O., and Ginsberg, M. H. (1999) *J. Biol. Chem.* **274,** 28071–28077
13. Bennett, J. S., Zigmond, S., Vilaire, G., Cunningham, M. E., and Bednar, B. (1999) *J. Biol. Chem.* **274,** 25301–25307
14. Law, D. A., Nannizzi-Alaimo, L., and Phillips, D. R. (1996) *J. Biol. Chem.* **271,** 10811–10815
15. Chen, Y.-P., O'Toole, T. E., Leong, L., Liu, B.-Q., Diaz-Gonzalez, F., and Ginsberg, M. H. (1995) *Blood* **86,** 2606–2615
16. Komatsu, N., Kunitama, M., Hagiwara, T., Kato, T., Miyazaki, H., Eguchi, M., Yamamoto, M., and Miura, Y. (1996) *Blood* **87,** 4552–4560
17. Sato, T., Fuse, A., Eguchi, M., Hayashi, Y., Ryo, R., Adachi, M., Kishimoto, Y., Teramura, M., Mizoguchi, H., Shima, Y., Komori, I., Sunami, S., Okimoto, Y., and Nakajima, H. (1989) *Br. J. Haematol.* **72,** 184–190
18. Rose, M., and Botstein, D. (1983) *Methods Enzymol.* **101,** 167–180
19. Scatchard, G. (1949) *Ann. N. Y. Acad. Sci.* **51,** 660–672
20. Jang, W., Weber, J. S., Bashir, R., Bushby, K., and Meisler, M. H. (1996) *Genomics* **36,** 366–368
21. Hu, R.-M., Han, Z.-G., Song, H.-D., Peng, Y.-D., Huang, Q.-H., Ren, S.-H., Gu, Y.-J., Huang, C.-H., Li, Y.-B., Jiang, C.-L., Fu, G., Zhang, Q.-H., Gu, B.-W., Dai, M., Mao, Y.-F., Gao, G.-F., Rong, R., Ye, M., Zhou, J., Xu, S.-H., Gu, J., Shi, J.-X., Jin, W.-R., Zhang, C.-K., Wu, T.-M., Huang, G.-Y., Chen, Z., Chen, M.-D., and Chen, J.-L. (2000) *Proc. Natl. Acad. Sci. U. S. A.* **97,** 9543–9548
22. Solski, P. A., Quilliam, L. A., Coats, S. G., Der, C. J., and Buss, J. E. (1995) *Methods Enzymol.* **250,** 435–454
23. Ponting, C. P. (2000) *Biochem. J.* **351,** 527–535
24. Biederer, T., Volkwein, C., and Sommer, T. (1997) *Science* **278,** 1806–1809
25. Burns, K., Clatworthy, J., Martin, L., Martinon, F., Plumpton, C., Maschera, B., Lewis, A., Ray, K., Tschopp, J., and Volpe, F. (2000) *Nat. Cell Biol.* **2,** 346–351
26. Takeyasu, G., Kishida, S., Hiyama, A., Yamaguchi, K., Shibuya, H., Irie, K., Nomiyama-Tsuji, J., and Matsumoto, K. (2000) *Mol. Cell* **5,** 649–658
27. Bion, S., D'Adamo, P., Maestrini, E., Gedeon, A. K., Bolhuis, P. A., and Toniolo, D. (1996) *Nat. Genet.* **12,** 385–389

28. Neuwald, A. F. (1997) *Curr. Biol.* **7,** R465–R466
29. Barth, P. G., Scholte, H. R., Berden, J. A., Moorsel, J. M. V. D. K.-V., and Sobotka-Plojhar, M. A. (1983) *J. Neurol. Sci.* **62,** 327–355
30. Moolenaar, W. H. (1995) *J. Biol. Chem.* **270,** 12949–12952
31. English, D., Cui, Y., and Siddiqui, R. A. (1996) *Chem. Phys. Lipids* **80,** 117–132
32. West, J., Tompkins, C. K., Balantac, N., Nudelman, E., Meengs, B., White, T., Bursten, S., Coleman, J., Kumar, A., Singer, J. W., and Leung, D. W. (1997) *DNA Cell Biol.* **16,** 691–701
33. Smyth, S. S., Hillerry, C. A., and Parise, L. V. (1992) *J. Biol. Chem.* **267,** 15568–15577
34. Vila, M. d. C., Milligan, G., Standaert, M. L., and Farese, R. (1990) *Biochemistry* **29,** 8735–8740
35. Taniguchi, T., Kitagawa, H., Yasue, S., Yanagi, S., Sakai, K., Asahi, M., Ohta, S., Takeuchi, F., Nakamura, S., and Yamamura, H. (1993) *J. Biol. Chem.* **268,** 2277–2279
36. Fox, J. E. B. (2001) *Thromb. Haemostasis* **86,** 198–213

5. Adlkofer K, Martini R, Aguzzi A, et al. Hypermyelination and demyelinating peripheral neuropathy in PMP-22-deficient mice. Nat Genet 1995;11:274–280.
6. Kamholz J, Menichella D, Jani A, et al. Charcot-Marie-Tooth disease type 1: molecular pathogenesis to gene therapy. Brain 2000;123:222–233.
7. Amato AA, Gronseth GS, Callerame KJ, et al. Tomaculous neuropathy: a clinical and electrophysiological study in patients with and without 1.5-Mb deletions in chromosome 17p11.2. Muscle Nerve 1996;19:16–22.
8. Andersson PB, Yuen E, Parko K, et al. Electrodiagnostic features of hereditary neuropathy with liability to pressure palsies. Neurology 2000;54:40–44.
9. Infante J, Garcia A, Combarros O, et al. Diagnostic strategy for familial and sporadic cases of neuropathy associated with 17p12.2 deletion. Muscle Nerve 2001;24:1149–1155.
10. Mouton P, Tardieu S, Gouider R, et al. Spectrum of clinical and electrophysiologic features in HNPP patients with the 17p11.2 deletion. Neurology 1999;52:1440–1446.
11. Pareyson D, Scaioli V, Taroni F, et al. Phenotypic heterogeneity in hereditary neuropathy with liability to pressure palsies associated with chromosome 17p11.2–12 deletion. Neurology 1996;46:1133–1137.
12. Lewis RA, Sumner AJ, Shy ME, et al. Electrophysiological features of inherited demyelinating neuropathies: a reappraisal in the era of molecular diagnosis. Muscle Nerve 2000; 23:1472–1487.
13. Gouider R, LeGuern E, Gugenheim M, et al. Clinical, electrophysiologic, and molecular correlations in 13 families with hereditary neuropathy with liability to pressure palsies and a chromosome 17p11.2 deletion. Neurology 1995; 45:2018–2023.
14. Madrid R, Bradley WG. The pathology of neuropathies with focal thickening of the myelin sheath (tomaculous neuropathy), studies on the formation of the abnormal myelin sheath. J Neurol Sci 1975;25:415–448.
15. Yoshikawa H, Dyck PJ. Uncompacted inner myelin lamellae in inherited tendency to pressure palsy. J Neuropathol Exp Neurol 1991;50:649–657.
16. Dawson DM, Hallett M, Wilbourn AJ. Entrapment neuropathies. 3rd ed. Philadelphia: Lippincott–Raven, 1999.

Clinicopathological features of genetically confirmed Danon disease

K. Sugie, MD, PhD; A. Yamamoto, MD; K. Murayama, BS; S.J. Oh, MD; M. Takahashi, MD; M. Mora, MD; J.E. Riggs, MD; J. Colomer, MD; C. Iturriaga, MD; A. Meloni, MD; C. Lamperti, MD; S. Saitoh, MD, PhD; E. Byrne, MD, DSc; S. DiMauro, MD; I. Nonaka, MD, PhD; M. Hirano, MD; and I. Nishino, MD, PhD

Abstract—*Background*: Danon disease is due to primary deficiency of lysosome-associated membrane protein-2. *Objective*: To define the clinicopathologic features of Danon disease. *Methods*: The features of 20 affected men and 18 affected women in 13 families with genetically confirmed Danon disease were reviewed. *Results*: All patients had cardiomyopathy, 18 of 20 male patients (90%) and 6 of 18 female patients (33%) had skeletal myopathy, and 14 of 20 male patients (70%) and one of 18 female patients (6%) had mental retardation. Men were affected before age 20 years whereas most affected women developed cardiomyopathy in adulthood. Muscle histology revealed basophilic vacuoles that contain acid phosphatase–positive material within membranes that lack lysosome-associated membrane protein-2. Heart transplantation is the most effective treatment for the otherwise lethal cardiomyopathy. *Conclusions*: Danon disease is an X-linked dominant multisystem disorder affecting predominantly cardiac and skeletal muscles.

NEUROLOGY 2002;58:1773–1778

Danon disease, an X-linked cardioskeletal myopathy originally reported as "lysosomal glycogen storage disease with normal acid maltase,"[1] is caused by primary deficiency of lysosome-associated membrane protein-2 (LAMP-2), a major lysosomal membrane protein.[2] Together with its paralogous counterpart LAMP-1, LAMP-2 is a highly glycosylated protein coating the inner side of the lysosomal membrane. The *LAMP-2* gene is located on Xq24.[3] LAMP-2 is thought to protect the lysosomal membrane from proteolytic enzymes within lysosomes and to act as a receptor for proteins to be imported into lysosomes.[4] However, the precise functional role of LAMP-2 is still controversial.

Danon disease is characterized clinically by the triad of cardiomyopathy, myopathy, and mental re-

From the Departments of Ultrastructural Research (Drs. Sugie, Yamamoto, Nonaka, and Nishino, and K. Murayama) and Neuromuscular Research (Dr. Nishino), National Institute of Neuroscience, National Center of Neurology and Psychiatry, Kodaira, Tokyo, Japan; the Department of Neurology (Dr. Sugie), Nara Medical University, Kashihara, Nara, Japan; the Department of Neurology (Dr. Oh), University of Alabama at Birmingham; the Department of Pediatrics (Drs. Takahashi and Saitoh), Hokkaido University, Sapporo, Hokkaido, Japan; the Department of Neuromuscular Diseases (Dr. Mora), National Neurological Institute "C. Besta," Milan, Italy; the Department of Neurology (Dr. Riggs), West Virginia University, Morgantown; Hospital Sant Joan de Déu (Drs. Colomer and Iturriaga), Barcelona, Spain; the Department of Pediatrics (Dr. Meloni), University of Cagliari, Italy; the Department of Clinical Neurosciences (Dr. Byrne), St. Vincent's Hospital, Fitzroy, Australia; and the Department of Neurology (Drs. Lamperti, DiMauro, and Hirano), Columbia University, New York, NY.

Supported in part by the Research Grant (11B-1) for Nervous and Mental Disorders from the Ministry of Health and Welfare.

Received November 5, 2001. Accepted in final form March 14, 2002.

Address correspondence and reprint requests to Dr. Ichizo Nishino, Department of Neuromuscular Research, National Institute of Neuroscience, National Center of Neurology and Psychiatry, 4-1-1 Ogawahigashi-cho, Kodaira, Tokyo 187-8502, Japan; e-mail: nishino@ncnp.go.jp

Table 1 Summary of 13 families with Danon disease

Family	Ethnic background	Site of *LAMP-2* gene mutation	Affected men	Affected women	Study
1	Japanese	E9b	Proband, 1 cousin	Mother, 1 sister	9, 12
2	Japanese	E4	Proband	—	16
3	Japanese	I6*	Proband	Mother	3, 11
4	Italian	E8	Proband, 1 nephew	Mother, 1 sister	10
5	Afro-American	E8	Proband	Mother, 1 grandmother	
6	Japanese	I5	Proband	—	
7	Afro-American	I5	Proband	Mother, 2 sisters	7
8	Anglo-Saxon	I5	Proband, 1 brother	Mother	4
9	Japanese	I5/E6 junction	Proband	Mother	
10	Greek	E1	Proband, 2 cousins	Mother, 1 aunt	14
11	Japanese	E7	Proband	1 Sister	
12	Spanish	E2	Proband, 2 cousins	Mother, 1 grandmother, 1 aunt	
13	Italian	E4	Proband	—	

* Exon skipping mutation.

tardation.[1,5,6] Muscle biopsy reveals small autophagic vacuoles in muscle fibers. Some of these vacuoles have features of plasma membrane.[7] Diagnosis had been based on these clinical and histologic features in addition to normal acid maltase activity in skeletal muscle. However, disorders reported as "lysosomal glycogen storage disease with normal acid maltase" are genetically heterogeneous. In fact, two patients reported to have an infantile form of Danon disease did not have LAMP-2 deficiency.[8]

To better delineate the clinicopathologic features of Danon disease, we studied 38 patients from 13 families with genetically confirmed Danon disease.

Materials and methods. *Patients.* We reviewed the clinicopathologic features of 20 affected men and 18 affected women from 13 families with genetically confirmed Danon disease. Immunohistochemistry, Western blot analyses, or both confirmed LAMP-2 deficiency in all specimens. Clinical manifestations of seven of the 13 families were reported previously.[1,5,6,9-14] Statistical values are expressed as mean ± SD.

Sequence analysis. The open reading frame of the *LAMP-2* gene consists of nine exons. Human exon 9 exists in two forms, exon 9a and 9b, that are alternatively spliced and processed into two isoforms, *LAMP-2a* and *LAMP-2b*.[15] We sequenced the entire coding region, including both exons 9a and 9b, and the exon/intron junctions of the *LAMP-2* gene as described.[2]

Muscle biopsy. Muscle biopsy was performed in all probands. Biopsy specimens were either frozen in liquid nitrogen–cooled isopentane for histochemistry or fixed with glutaraldehyde for electron microscopy. Transverse serial frozen sections of 10-μm thickness were stained with hematoxylin and eosin, modified Gomori trichrome, and a battery of histochemical methods.

In addition, we performed indirect immunofluorescence staining on 6-μm cryosections of muscle using mouse monoclonal antibodies according to methods described previously.[16] These sections were incubated at 37 °C for 2 hours with the primary mouse IgG antibodies against LAMP-2 (H4B4, Developmental Studies Hybridoma Bank, Iowa City, IA), the C-terminal of dystrophin (NCL-DYS2, Novocastra, Newcastle Upon Tyne, UK), laminin α2 (NCL-MEROSIN, Novocastra), and α-sarcoglycan (NCL-α-SARC, Novocastra). They were subsequently incubated at 37 °C for 1 hour with a secondary antibody fluorescein isothiocyanate–labeled goat F(ab')2 antimouse IgG (M102, Leinco Technology, St. Louis, MO). All sections were examined by fluorescence microscopy. Control specimens were obtained from 10 patients with morphologically normal muscle.

For electron microscopy, biopsy specimens were fixed in buffered 2% isotonic glutaraldehyde at pH 7.4, postfixed in osmium tetroxide, and embedded in epoxide resin. Ultrathin sections were stained with uranyl acetate and lead nitrate and examined with an H-7000 electron microscope (Hitachi). When sufficient tissues was available, we also performed Western blot analysis.

Results. *LAMP-2 gene mutations.* We identified *LAMP-2* mutations in all of the probands and affected family members from whom samples were available (table 1).[5] All mutations were either nonsense or frame-shift mutations that are predicted to cause truncation of the protein, except for the exon 6 skipping mutation in Family 3.[5]

Protein analysis. On immunohistochemical analysis, LAMP-2 staining was completely absent in muscle of the probands. By Western blot analysis, LAMP-2 was undetectable except for the proband in Family 1 who showed a small amount of LAMP-2 protein, as reported previously.[5]

Clinical features. The clinical features in 20 male patients with Danon disease are summarized in table 2. All 13 probands were male. The two most common features were cardiomyopathy and myopathy; mental retardation was present in 14 of the 20 male patients.

Ages at onset in the 20 male patients varied from 10 months to 19 years. Onset may be earlier but may go undetected because of the subacute nature and slow pro-